



CERN-EP-2022-283
12 December 2022

First measurement of prompt and non-prompt D^{*+} vector meson spin alignment in pp collisions at $\sqrt{s} = 13$ TeV

ALICE Collaboration*

Abstract

This letter reports the first measurement of spin alignment, with respect to the helicity axis, for D^{*+} vector mesons and their charge conjugates from charm-quark hadronisation (prompt) and from beauty-meson decays (non-prompt) in hadron collisions. The measurements were performed at midrapidity ($|y| < 0.8$) as a function of transverse momentum (p_T) in proton–proton (pp) collisions collected by ALICE at the centre-of-mass energy $\sqrt{s} = 13$ TeV. The diagonal spin density matrix element ρ_{00} of D^{*+} mesons was measured from the angular distribution of the $D^{*+} \rightarrow D^0(\rightarrow K^- \pi^+) \pi^+$ decay products, in the D^{*+} rest frame, with respect to the D^{*+} momentum direction in the pp centre of mass frame. The ρ_{00} value for prompt D^{*+} mesons is consistent with $1/3$, which implies no spin alignment. However, for non-prompt D^{*+} mesons an evidence of ρ_{00} larger than $1/3$ is found. The measured value of the spin density element is $\rho_{00} = 0.455 \pm 0.022(\text{stat.}) \pm 0.035(\text{syst.})$ in the $5 < p_T < 20$ GeV/ c interval, which is consistent with a PYTHIA 8 Monte Carlo simulation coupled with the EVTGEN package, which implements the helicity conservation in the decay of D^{*+} meson from beauty mesons. In non-central heavy-ion collisions, the spin of the D^{*+} mesons may be globally aligned with the direction of the initial angular momentum and magnetic field. Based on the results for pp collisions reported in this letter it is shown that alignment of non-prompt D^{*+} mesons due to the helicity conservation coupled to the collective anisotropic expansion may mimic the signal of global spin alignment in heavy-ion collisions.

arXiv:2212.06588v2 [nucl-ex] 11 Oct 2023

*See Appendix A for the list of Collaboration members

1 Introduction

The production of hadrons containing heavy quarks, i.e. charm and beauty, has been extensively studied in both lepton and hadron collisions, improving significantly the understanding of the hadronisation mechanism [1–8]. However, several aspects of the transition of the heavy quark to the final-state hadron are not yet settled. One of them regards the spin properties of produced particles in the quark hadronisation. In the limit of very large heavy-quark mass ($m_Q \rightarrow \infty$), the polarisation of heavy-flavour baryons is assumed to be that carried by the heavy valence quark [9]. This assumption was studied at LEP in e^+e^- collisions where the polarisation of Λ_b^0 baryons was used to probe the electroweak structure of the Z^0 boson production and decays [10–14]. In hadronic collisions, the polarisation of Λ_b^0 baryons can arise during the hadronisation process if beauty quarks are produced with a transverse polarisation, as predicted by the heavy-quark effective theory [9, 11]. At this time, one measurement, performed by the LHCb Collaboration, found no significant polarisation [15]. For vector mesons with quantum numbers $J^P = 1^-$, both in lepton and hadron collisions, at least part of the polarisation should arise from the hadronisation process [9]. Models based on statistical quantum mechanics considerations [16, 17], heavy-quark effective theory [9], or inspired by quantum chromodynamics (QCD) [18] provide very different predictions, from no polarisation, to very large longitudinal or transverse polarisation. This aspect of the hadronisation is typically not accounted for in QCD-inspired Monte Carlo (MC) generators based on the Lund string model [19], such as PYTHIA 8 [20, 21], or the clustering model [22], as implemented in HERWIG 7 [23]. Measurements of excited B vector meson states in Z^0 decays at LEP did not show any significant polarisation [24, 25]. For charm vector mesons (D^{*+}) a longitudinal polarisation was observed by OPAL [26]. However, previous measurements in e^+e^- collisions indicated no significant polarisation for D^{*+} mesons [27–29].

The polarisation of vector mesons containing heavy quarks in heavy-ion collisions is of special interest. The initial stages of such collisions, with non-zero impact parameter, are expected to be characterised by a large orbital angular momentum [30] and a strong magnetic field [31–33]. These initial conditions could influence the produced colour-deconfined matter (called quark–gluon plasma [34, 35]). The directions of the angular momentum and the magnetic field in such collisions are perpendicular to the reaction plane (subtended by the beam axis and impact parameter) [36]. Theoretical calculations at LHC energies predict the values of the angular momentum to be of the order of $10^7 \hbar$ [30] and the magnetic field to be about 10^{16} T [31–33, 37, 38]. While the angular momentum, a conserved quantity in strong interactions, is expected to affect the whole evolution of the collision, the magnetic field is transient in nature and its strength falls steeply with time. Heavy quarks are produced at the initial stages of heavy-ion collisions, in a time scale shorter than the quark–gluon plasma formation time [39] and are sensitive to the large initial magnetic field as well as the angular momentum. In the presence of these initial conditions, charm quarks can be polarised. The quark polarisation is expected to be further transferred to the final-state hadrons during hadronisation and it is predicted to be different in the case of hadronisation in vacuum, or recombination with light quarks from the deconfined medium [36, 40–42]. Measurements in heavy-ion collisions indicate that the recombination mechanism is important to describe the production and angular anisotropies of charm hadrons [43–51]. If observed, a non-zero polarisation of D^{*+} mesons will be a manifestation of the angular momentum and the magnetic field created in heavy-ion collisions. The study of D^{*+} mesons would provide additional information, crucial for the interpretation of the recently measured J/ψ polarisation in Pb–Pb collisions by the ALICE Collaboration [52, 53]. In fact, the polarisation of D^{*+} and J/ψ mesons have different contributions from the angular momentum and the magnetic field, given the valence light quark present in the D^{*+} meson, which is expected to be less sensitive than the charm quark to the magnetic field. However, the interpretation of experimental data for heavy-ion collisions requires a baseline study in elementary proton–proton (pp) collisions, where such initial conditions are not expected to form. Moreover, in this study, one of the major sources of background is the feed-down contribution of D^{*+} mesons originating from decays of scalar mesons containing a beauty quark, which are observed to be longitudinally polarised by the Belle and LHCb

Collaborations in e^+e^- and pp collisions, respectively [54, 55]. This is a direct consequence of the helicity conservation and the Vector–Axial (V–A) nature of the weak interaction involved in the $b \rightarrow c$ decay, which leads to left-handed fermion couplings in interactions with W bosons [56, 57]. It is therefore important to separate contributions to the polarisation from promptly produced mesons and from those originating in beauty-hadron decays. This was not possible in the case of the J/ψ meson in Pb–Pb collisions with LHC Run 2 data, for which only the inclusive polarisation was used as baseline [53].

The polarisation of D^{*+} vector mesons cannot be probed directly as D^{*+} mesons are measured through the parity conserving strong decay $D^{*+} \rightarrow D^0(\rightarrow K^-\pi^+)\pi^+$. However, experimentally, the spin alignment along the quantisation direction can be studied by measuring the diagonal spin density matrix element (ρ_{00}) of the vector meson. The ρ_{00} reflects the probability of finding a vector meson in the state with spin zero out of possible states with spin projection -1 , 0 , and 1 [58]. If the spin of particles is homogeneously distributed, all spin states are expected to be equally probable, thereby yielding $\rho_{00} = 1/3$. The spin alignment is studied by measuring the angular distribution of the decay products of vector mesons. Their decay products are measured with respect to a quantisation axis, which is the vector meson momentum direction (helicity axis) in pp collisions and the perpendicular direction of the reaction plane in heavy-ion collisions. In the latter, these two axes are further correlated through the anisotropic collective expansion which is quantified by coefficients in a Fourier decomposition of the azimuthal-angle distribution of final-state particle momenta, with the second-harmonic coefficient v_2 , called elliptic flow [59], being the dominant one [50]. The angular distribution of the D^{*+} decay products is expressed as

$$\frac{dN}{d\cos\theta^*} \propto [1 - \rho_{00} + (3\rho_{00} - 1)\cos^2\theta^*], \quad (1)$$

where θ^* is the angle between the momentum of either the D^0 meson or the pion in the rest frame of the vector meson with respect to the quantisation axis [60].

In this letter, the first measurement of the spin alignment of D^{*+} mesons from charm-quark hadronisation (prompt) and from beauty-hadron decays (non-prompt) at midrapidity is presented as a function of transverse momentum (p_T) in pp collisions at a centre-of-mass energy of $\sqrt{s} = 13$ TeV. Based on these measurements, quantitative predictions for the spin distributions of non-prompt D^{*+} meson for a future measurement of the D^{*+} -meson spin alignment in heavy-ion collisions are provided.

2 Experimental apparatus and data analysis

The analysis was performed using about 1.8×10^9 minimum-bias and about 10^9 high-multiplicity triggered pp collisions at $\sqrt{s} = 13$ TeV recorded with the ALICE apparatus [61, 62], corresponding to an integrated luminosity of $\mathcal{L}_{\text{int}} \approx 32 \text{ nb}^{-1}$ and $\mathcal{L}_{\text{int}} \approx 7.7 \text{ pb}^{-1}$, respectively. The minimum-bias trigger required coincident signals in the two V0 detectors, which are two scintillator arrays covering the pseudorapidity intervals $-3.7 < \eta < -1.7$ and $2.8 < \eta < 5.1$ [63]. The high-multiplicity trigger selected the 0.17% highest-multiplicity events out of all inelastic collisions with at least one charged particle in the pseudorapidity range $|\eta| < 1$, relying on the signal amplitudes of the V0 detectors. Events were further selected offline to remove machine-induced backgrounds [61]. They were required to have a reconstructed collision vertex located within ± 10 cm from the centre of the detector along the beam-line direction to maintain a uniform acceptance. Events with multiple reconstructed primary vertices (pileup) were rejected. Primary vertices were reconstructed from track segments measured with the two innermost layers of the Inner Tracking System (ITS), which consists of six cylindrical layers of silicon detectors [64]. The remaining undetected pileup was studied and found to be negligible for this analysis.

The D^{*+} mesons and their charge conjugates were measured at midrapidity ($|y| < 0.8$) via the $D^{*+} \rightarrow D^0(\rightarrow K^-\pi^+)\pi^+$ decay channel, with branching ratio $\text{BR} = (2.67 \pm 0.03)\%$ [65]. The measurement of D^{*+} mesons was based on charged-particle tracks reconstructed with the Time Projection Chamber (TPC) [66] and ITS detectors. The D^0 decay candidates were defined combining pairs of tracks with

the expected charge combinations. Each track from the decay was required to have $|\eta| < 0.8$, $p_T > 0.3$ GeV/ c , at least 70 (out of 159) associated space points in the TPC, and a minimum of two hits in the ITS, with at least one in either of the two innermost layers to ensure a good pointing resolution. The D^{*+} -meson candidates were reconstructed by combining D^0 candidates with low- p_T tracks (referred to as soft pions) having $|\eta| < 0.8$, $p_T > 50$ MeV/ c , and at least two hits in the ITS. The analysis was based on the reconstruction of decay-vertex topologies of D^0 mesons displaced from the interaction vertex. In particular, the proper decay length of D^0 mesons of $c\tau \approx 123$ μm and that of beauty hadrons of $c\tau \approx 500$ μm were exploited to resolve the D^0 -meson decay vertices. In order to reduce the large combinatorial background and to separate the contribution of prompt and non-prompt D^{*+} mesons, a multiclass classification algorithm based on Boosted Decision Trees (BDTs) was used [67, 68]. The candidate information used by the BDT algorithm to distinguish among prompt and non-prompt D^{*+} mesons and background candidates was based on i) the distance between the reconstructed D^0 -meson decay vertex and the primary vertex, ii) the D^0 -meson and soft-pion distance of closest approach to the interaction vertex, iii) the cosine of the pointing angle between the D^0 -meson candidate line of flight and its reconstructed momentum vector, and iv) the particle identification (PID) information of the decay tracks. The PID information was provided by the specific energy loss and the flight time of particles measured with the TPC and Time Of Flight (TOF) [69] detectors, respectively. Signal samples of prompt and non-prompt D^{*+} mesons for the BDT training were obtained from MC simulations based on the PYTHIA 8.243 event generator [20, 21] with the Monash tune [70] and GEANT 3 package [71] for the propagation of the generated particles through the detector. The background samples were obtained in data from the sideband region of the invariant-mass distribution $\Delta M = M(K\pi\pi) - M(K\pi)$. The sideband region was chosen as the invariant-mass interval $\Delta M > 150$ MeV/ c^2 , where no D^{*+} signal is present. Independent BDTs were trained for the high-multiplicity and minimum-bias samples in three different p_T intervals, i.e. $5 < p_T < 7$ GeV/ c , $7 < p_T < 10$ GeV/ c , and $10 < p_T < 20$ GeV/ c . Subsequently, they were applied to the real data sample in which the type of candidate is unknown. The BDT outputs are related to the candidate probability to be a prompt D^{*+} meson, non-prompt D^{*+} meson, or combinatorial background.

The selection based on the probability to be background was optimised to yield a good statistical significance and purity of the signal. By selecting high probability to be prompt or non-prompt D^{*+} mesons, the samples of candidates were further separated to the charm-enhanced (significant contribution of prompt D^{*+} mesons) and the beauty-enhanced (significant contribution of non-prompt D^{*+} mesons) samples. The threshold values were tuned as a function of p_T using MC simulations. The fractions of prompt (f_{prompt}) and non-prompt ($f_{\text{non-prompt}}$) D^{*+} mesons in each sample were evaluated with a data-driven method based on the sampling of the raw yield Y_i at different values of the BDT-output score related to the probability of being a non-prompt D^{*+} meson. These fractions can be computed by solving a system of equations that relate raw yields to the corrected yields of prompt (N_{prompt}) and non-prompt ($N_{\text{non-prompt}}$) D^{*+} mesons by the product of the geometrical acceptance and the reconstruction and selection (including BDT) efficiency factors ($\text{Acc} \times \varepsilon$) for prompt and non-prompt D^{*+} mesons. Each equation, obtained for a set of BDT selections i , can be expressed as

$$(\text{Acc} \times \varepsilon)_{\text{prompt},i} \times N_{\text{prompt}} + (\text{Acc} \times \varepsilon)_{\text{non-prompt},i} \times N_{\text{non-prompt}} - Y_i = \delta_i, \quad (2)$$

where δ_i is the residual originating from the uncertainties on Y_i , $(\text{Acc} \times \varepsilon)_{\text{non-prompt},i}$, and $(\text{Acc} \times \varepsilon)_{\text{prompt},i}$. To define the sets of selections, the BDT-output response related to the probability of a candidate to be a non-prompt D^{*+} meson was sampled monotonically, to obtain n selections ordered in such a way that the i^{th} selected sample was completely included in the $(i-1)^{\text{th}}$ one. The system of equation is then solved via a χ^2 minimisation, which provides as output the corrected yields of prompt (N_{prompt}) and non-prompt ($N_{\text{non-prompt}}$) D^{*+} mesons and their covariance matrix. A detailed description of this method is presented in Refs. [72–74]. For each p_T interval, the raw yields of D^{*+} mesons were extracted with a fit to the distribution of the invariant mass ΔM .

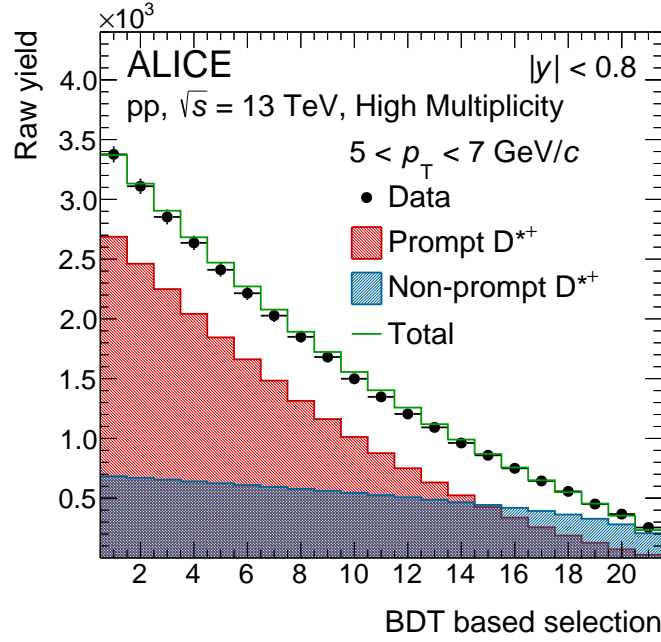


Figure 1: Raw yield as a function of the BDT selection and extracted contributions from prompt and non-prompt D^{*+} mesons with $5 < p_T < 7$ GeV/ c and $|y| < 0.8$ in the high-multiplicity triggered pp collisions at $\sqrt{s} = 13$ TeV.

The distribution was fitted with a combination of the Gaussian function corresponding to the D^{*+} signal and a background function. The shape of the background distribution can be described with the function $p_0 \sqrt{\Delta M - M_\pi} e^{p_1(\Delta M - M_\pi)}$, where p_0 and p_1 are free parameters and M_π is the pion mass. The corresponding $\text{Acc} \times \epsilon$ factors were obtained with MC simulations analogous to those used for the BDT trainings. Finally, the fraction of (non-)prompt D^{*+} mesons for a given set of selections was computed as

$$f_{(\text{non-})\text{prompt},j} = \frac{(\text{Acc} \times \epsilon)_{(\text{non-})\text{prompt},j} \times N_{(\text{non-})\text{prompt}}}{(\text{Acc} \times \epsilon)_{\text{prompt},j} \times N_{\text{prompt}} + (\text{Acc} \times \epsilon)_{(\text{non-})\text{prompt},j} \times N_{(\text{non-})\text{prompt}}}. \quad (3)$$

A different index "j" is used here to underline the fact that not all of these sets are used for the χ^2 minimisation given by Eq. 2. The uncertainty of $f_{(\text{non-})\text{prompt},j}$ is computed considering the covariance matrix of N_{prompt} and $N_{(\text{non-})\text{prompt}}$ obtained in the χ^2 -minimisation procedure. Figure 1 shows an example of a raw-yield extracted as a function of the BDT selection employed in the minimisation procedure for D^{*+} mesons with $5 < p_T < 7$ GeV/ c in high-multiplicity triggered pp collisions at $\sqrt{s} = 13$ TeV. The leftmost data point of the distribution is the raw yield corresponding to the loosest selection on the BDT output related to the candidate probability of being a non-prompt D^{*+} meson, while the rightmost one corresponds to the strictest selection, which is expected to preferentially select non-prompt D^{*+} mesons. The $\text{Acc} \times \epsilon$ factors obtained for these selections ranged from about 10% to 0.1% for prompt D^{*+} mesons, and from about 30% to 10% for non-prompt D^{*+} mesons. The prompt and non-prompt components are represented by the red and blue filled histograms, respectively, while their sum is depicted by the green histogram. The f_{prompt} factor obtained in the charm-enhanced sample is higher than 90% for both the high-multiplicity and minimum-bias triggered events, while the $f_{\text{non-prompt}}$ in the beauty-enhanced sample is $\sim 60\%$ and $\sim 40\%$ almost independent of p_T for high-multiplicity and minimum-bias triggered events, respectively.

The raw yields of D^{*+} mesons were extracted in different $\cos \theta^*$ and p_T intervals for both the beauty- and the charm-enhanced samples. Figure 2 shows the ΔM distributions in $5 < p_T < 7$ GeV/ c and $0.0 < \cos \theta^* < 0.2$ intervals for the beauty- and charm-enhanced samples in high-multiplicity triggered pp collisions at $\sqrt{s} = 13$ TeV. The width of the Gaussian function for the D^{*+} signal was fixed to the value

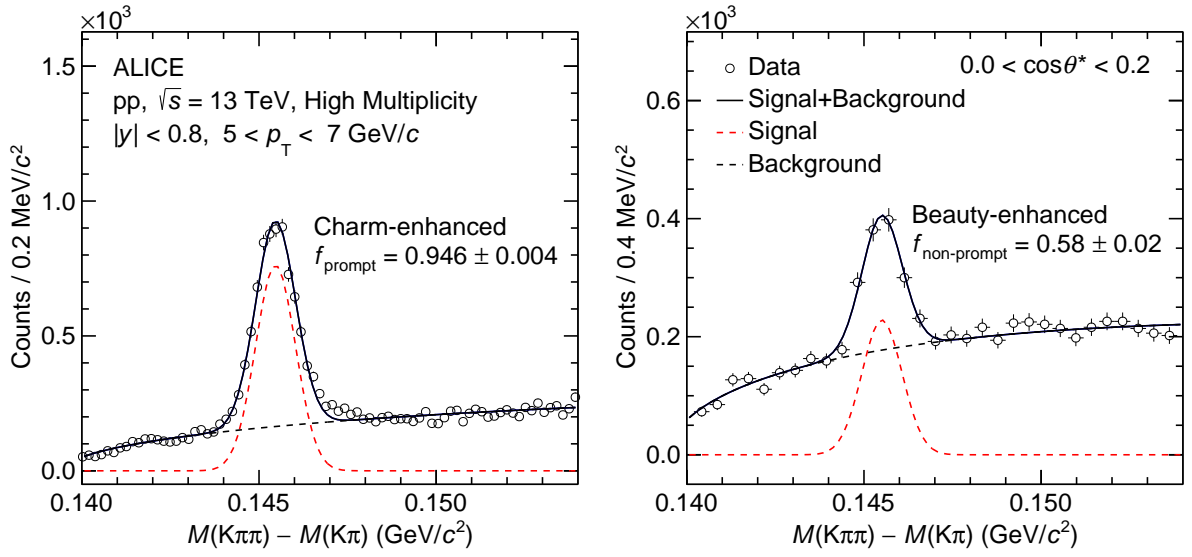


Figure 2: Invariant-mass distributions ΔM for the charm-enhanced (left panel) and the beauty-enhanced (right panel) samples in pp collisions at $\sqrt{s} = 13$ TeV, selected with the high-multiplicity trigger. The distributions are obtained at midrapidity ($|y| < 0.8$) in $5 < p_T < 7$ GeV/ c and $0.0 < \cos\theta^* < 0.2$.

from the MC simulation.

The raw yields were corrected for the corresponding $\text{Acc} \times \varepsilon$ factors in each $\cos\theta^*$ and p_T intervals. The

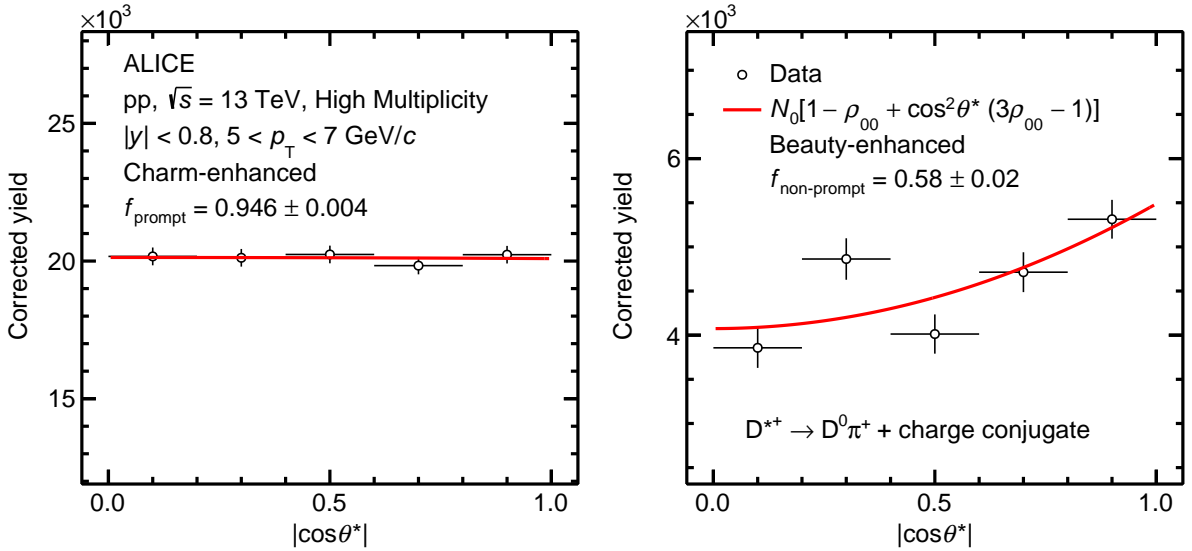


Figure 3: Acceptance and efficiency corrected angular distributions of the decay product in the rest frame of the D^{*+} meson with respect to the helicity axis. The left panel shows the angular distribution for the charm-enhanced D^{*+} sample in pp collisions at $\sqrt{s} = 13$ TeV, selected with the high-multiplicity trigger and the right panel shows the same but for the beauty-enhanced D^{*+} sample. The distributions are obtained at midrapidity ($|y| < 0.8$) in $5 < p_T < 7$ GeV/ c and are fitted with Eq. 1 to extract the ρ_{00} values. Only statistical uncertainties are shown.

impact on the ρ_{00} measurement due to the shape of the $\cos\theta^*$ and p_T distributions in the MC simulations was studied by weighting the generated MC distributions in order to reproduce the measured $\cos\theta^*$ and p_T distributions, and the effect on the $\text{Acc} \times \varepsilon$ values was found to be smaller than 0.1% in the analysed p_T intervals. The efficiency and acceptance corrected angular distributions at midrapidity for the selected p_T interval in high-multiplicity triggered pp collisions at $\sqrt{s} = 13$ TeV are shown in Fig. 3. The left panel of Fig. 3 shows the angular distribution of the charm-enhanced D^{*+} sample and the right panel shows the same but for the beauty-enhanced D^{*+} sample. The absolute value of $\cos\theta^*$ was considered due to the limited size of the analysed sample. The angular distributions were further fitted with the functional form given in Eq. 1 to extract the ρ_{00} values for both the charm- and the beauty-enhanced samples in each p_T interval.

It was verified with a MC simulation that the ρ_{00} parameter linearly depends on the fraction of non-prompt D^{*+} meson in the analysed sample. Hence, a linear fit of the measured ρ_{00} parameters obtained for the charm- and beauty-enhanced samples as a function of the $f_{\text{non-prompt}}$ was performed to obtain the ρ_{00} values for prompt and non-prompt D^{*+} mesons. The charm- and the beauty-enhanced selections used in this analysis provided two samples of independent candidates. Moreover, the samples of candidates in the minimum-bias and high-multiplicity triggered events are statistically independent. Considering that the measured ρ_{00} parameter can be decomposed as a linear combination of the prompt and non-prompt components,

$$\rho_{00} = f_{\text{prompt}} \times \rho_{00}^{\text{prompt}} + f_{\text{non-prompt}} \times \rho_{00}^{\text{non-prompt}}, \quad (4)$$

the four independent measurements corresponding to the charm- and beauty-enhanced samples for both minimum-bias and high-multiplicity events were fitted with a linear function in order to extrapolate it to $f_{\text{non-prompt}} = 0$ and $f_{\text{non-prompt}} = 1$. A similar procedure was adopted in Ref. [75] to measure the elliptic flow of prompt and non-prompt D mesons. With the current data samples it is not possible to perform the linear extrapolation of the ρ_{00} parameter independently for the minimum-bias and high-multiplicity collisions, which may have different physical origin, and the reported results are for the combined sample. Figure 4 shows the linear fit of ρ_{00} as a function of $f_{\text{non-prompt}}$ in $5 < p_T < 7$ GeV/c. The filled (empty) markers correspond to the measurements performed in the minimum-bias (high-multiplicity) pp collisions. The coloured band represents the 1σ confidence interval obtained from the linear fit. The ρ_{00} parameter for prompt and non-prompt D^{*+} mesons is then obtained by evaluating the fit function for $f_{\text{non-prompt}} = 0$ and $f_{\text{non-prompt}} = 1$, respectively.

3 Systematic uncertainties

There are four major sources of systematic uncertainties in the measurement of ρ_{00} for prompt and non-prompt D^{*+} mesons. These uncertainties are related to: i) the signal extraction, ii) the track reconstruction and selection efficiencies, iii) the BDT selection efficiency, and iv) the (non-)prompt fraction estimation. The systematic uncertainty arising from the signal extraction was estimated by varying the invariant-mass fit range, leaving the Gaussian width free in the fit, and using a bin-counting method for the raw-yield extraction. In the bin-counting method the signal yield is extracted by integrating the invariant-mass distribution after subtracting the background estimated from the background fit function. The systematic uncertainty associated with the track selection and reconstruction efficiency was evaluated by varying the track-quality selection criteria as described in Ref. [76]. The systematic uncertainty on the selection efficiency originates from imperfections in the description of the decay kinematics as well as the detector resolution and alignment in the simulation. It was estimated by comparing the ρ_{00} parameters obtained for prompt and non-prompt D^{*+} mesons with different BDT selection criteria. The uncertainty associated with the (non-)prompt fraction estimation was evaluated by varying the selection criteria described in Sec. 2, as well as the configuration of the invariant-mass fits. All of the above mentioned variations were performed independently and, assuming they are uncorrelated with each other, added in quadrature to obtain the total systematic uncertainties. Table 1 summarises the values of the

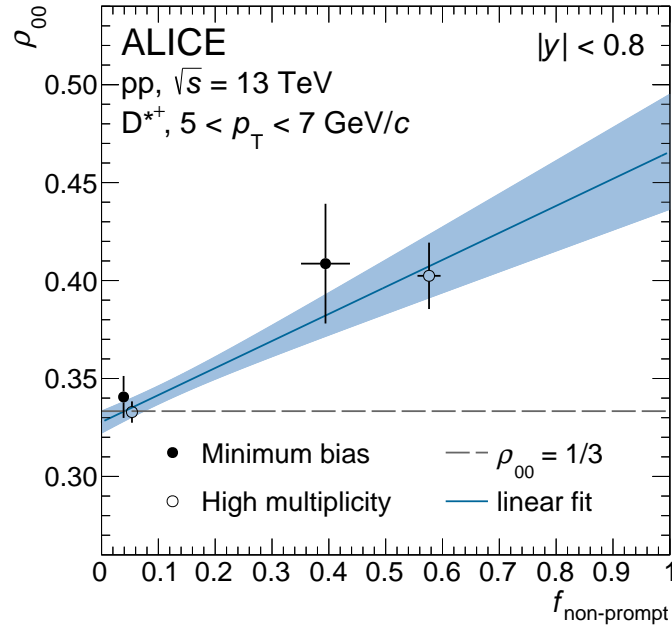


Figure 4: The spin density matrix element (ρ_{00}) as a function of $f_{\text{non-prompt}}$ in $5 < p_T < 7$ GeV/ c for charm- and beauty-enhanced samples obtained for minimum-bias and high-multiplicity triggered pp collisions at $\sqrt{s} = 13$ TeV. Only statistical uncertainties are shown. The blue line represents the linear fit to the data with the blue band indicating its 1σ confidence interval.

systematic uncertainties for the lowest and highest p_T intervals, reporting separately the various sources for prompt and non-prompt D^{*+} mesons. The total systematic uncertainty ranges between 2.5% and 3.5% for prompt D^{*+} mesons, and between 6.5% and 8% for non-prompt D^{*+} mesons. These systematic uncertainties were considered as fully correlated as a function of p_T .

In order to validate the results of the measurements, an additional analysis was performed with respect to a random quantisation axis (random unit vector direction in 3-dimensional space) which breaks the correlation between the helicity axis and the daughter momentum direction, due to helicity conservation. As expected, the extracted ρ_{00} values for both prompt and non-prompt D^{*+} mesons are consistent with $1/3$.

Table 1: Summary of the relative systematic uncertainties on the ρ_{00} parameter of prompt and non-prompt D^{*+} mesons for different p_T intervals.

p_T (GeV/ c)	Prompt		Non-prompt	
	5–7	10–20	5–7	10–20
Signal yield	2.0%	0.5%	4.0%	2.0%
Tracking efficiency	negl.	1.0%	2.0%	4.0%
BDT efficiency	0.5%	3.5%	6.0%	5.0%
(Non-)prompt fraction	negl.	negl.	0.5%	negl.
Total	2.5%	3.5%	8.0%	6.5%

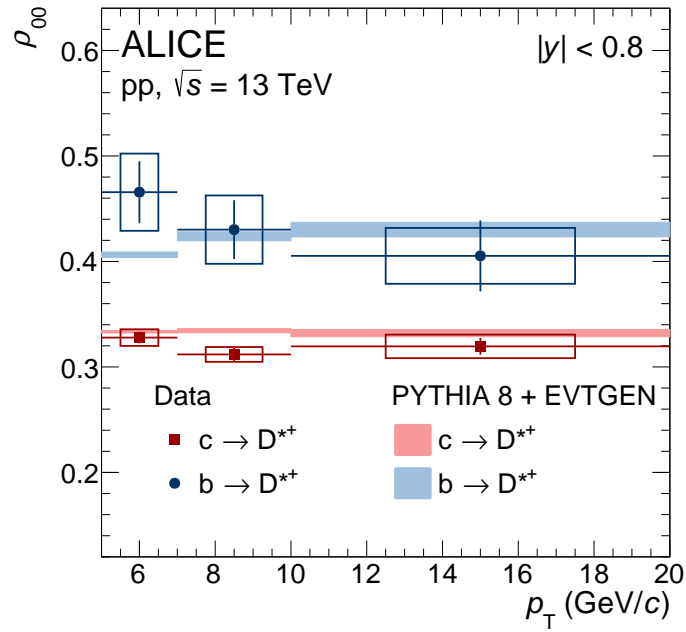


Figure 5: The spin density matrix element (ρ_{00}) for prompt and non-prompt D^{*+} mesons as a function of p_T in pp collisions at $\sqrt{s} = 13$ TeV. Measurements are carried out with respect to the helicity axis at $|y| < 0.8$. Statistical and systematic uncertainties are represented by bars and boxes, respectively. The measurements are compared with the estimations from the QCD-based MC event generator PYTHIA 8 + EVTGEN [70, 77]. Model estimations are shown by colour bands where the width of the band corresponds to the statistical uncertainty in model calculations.

4 Results

Figure 5 shows the ρ_{00} values with respect to the helicity axis for prompt and non-prompt D^{*+} mesons as a function of p_T in pp collisions at $\sqrt{s} = 13$ TeV. The measurements are performed in $|y| < 0.8$. The ρ_{00} values for prompt D^{*+} mesons are consistent with $1/3$, while for non-prompt D^{*+} mesons they are significantly larger than $1/3$ throughout the studied p_T range. The values measured in the three p_T intervals were averaged using the corrected yields of prompt and non-prompt D^{*+} mesons as weights. The resulting ρ_{00} values in the p_T interval between 5 and 20 GeV/c are

$$\begin{aligned}\rho_{00}(\text{prompt } D^{*+}) &= 0.324 \pm 0.004(\text{stat.}) \pm 0.008(\text{syst.}), \\ \rho_{00}(\text{non-prompt } D^{*+}) &= 0.455 \pm 0.022(\text{stat.}) \pm 0.035(\text{syst.}).\end{aligned}\tag{5}$$

This finding implies no spin alignment for prompt D^{*+} mesons with a simultaneous non-zero spin alignment of non-prompt D^{*+} mesons in high-energy pp collisions. The evidence of non-prompt D^{*+} -meson spin alignment can be understood as a consequence of helicity conservation in the decay of beauty scalar mesons to vector mesons. Measured ρ_{00} values are further compared with the MC event generator PYTHIA 8 + EVTGEN [70, 77]. The EVTGEN decay package, which conserves the helicity and account for the V–A nature in the decay of beauty mesons, is used in place of the default PYTHIA 8 decayer. In this case, model calculations are found to be in agreement with the extracted ρ_{00} values for both prompt and non-prompt D^{*+} mesons, while if the EVTGEN package is not used, the ρ_{00} parameter is found to be compatible with $1/3$ for both prompt and non-prompt D^{*+} mesons. The measured ρ_{00} for non-prompt D^{*+} mesons is qualitatively consistent with the longitudinal polarisation fraction (f_L) observed by the LHCb collaboration in the $B^0 \rightarrow D^{*-} D_s^{*+}$ decay with respect to a different quantisation axis defined by the B-meson momentum direction [55]. The direct comparison between the magnitudes of f_L and ρ_{00} measured by the LHCb and ALICE Collaborations is not possible due to the different quantisation axis

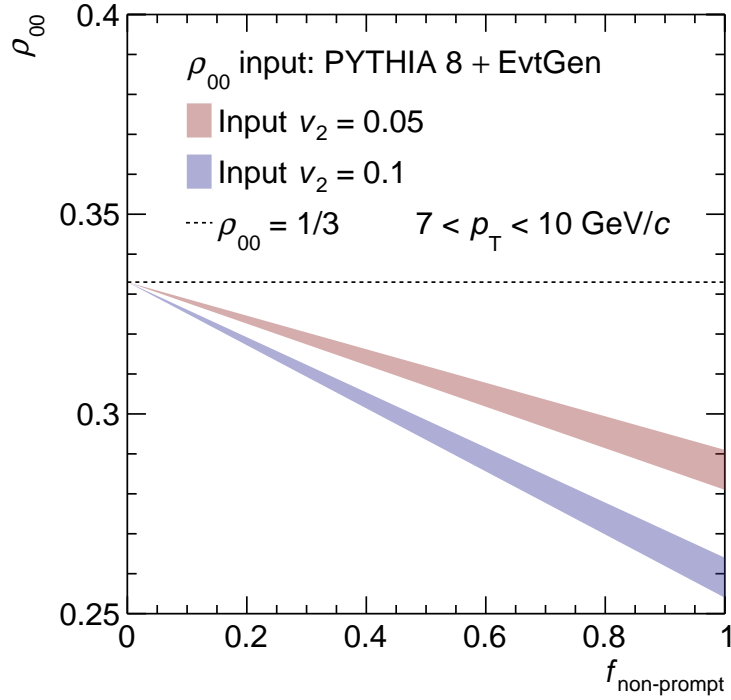


Figure 6: Model simulation based on the MC event generator PYTHIA 8 + EVTGEN [70, 77] for the spin density matrix element (ρ_{00}) for D^{*+} mesons with respect to the direction perpendicular to the reaction plane as a function of $f_{\text{non-prompt}}$. Model simulations are carried out for D^{*+} mesons at midrapidity ($|y| < 0.8$) with two input values of v_2 .

and the different decay channels. Therefore, dedicated model calculations are required for a quantitative comparison of the ALICE and LHCb data.

After the validation of the helicity conservation in the $H_b \rightarrow D^{*+} + X$ decays via the comparison with the measurement presented in this letter, the predicted ρ_{00} value obtained with PYTHIA 8 and the EVTGEN decay package can be used to estimate the magnitude of the corresponding contribution to the spin alignment in heavy-ion collisions. In particular, the spin alignment of non-prompt D^{*+} meson with respect to the helicity axis can affect the measurements of D^{*+} spin alignment with respect to the reaction plane in heavy-ion collisions. Due to the elliptic flow of the non-prompt D^{*+} mesons [50, 51, 78–80] in heavy-ion collisions, the helicity axis is correlated to the direction of the angular momentum and the magnetic field, which are perpendicular to the orientation of the reaction plane [50]. In order to obtain a quantitative estimate of this effect for heavy-ion collisions, a combination of PYTHIA 8 and the EVTGEN decay package, which are in good agreement with ALICE measurements as shown in Fig. 5, is used to model the spin alignment of non-prompt D^{*+} -mesons with respect to the helicity axis. Elliptic flow modulations of non-prompt D^{*+} mesons are introduced in the simulation by an appropriate rotation of the D^{*+} and its decay product momentum in the azimuthal plane. Introducing v_2 modulation aligns the momentum direction of non-prompt D^{*+} in the direction perpendicular to the reaction plane. Two different calculations with v_2 values of 0.05 and 0.1 were performed. These values were chosen to mimic measurements reported by the ALICE and ATLAS Collaborations of leptons from beauty-hadron decays for midcentral Pb–Pb collisions [81, 82]. Figure 6 shows the calculated ρ_{00} values for D^{*+} mesons as a function of $f_{\text{non-prompt}}$ with respect to the direction perpendicular to the reaction plane. It is found that in the presence of v_2 , helicity conservation in the beauty-meson decay leads to a value of ρ_{00} less than $1/3$. The opposite direction with respect to $1/3$ compared to the measurement presented in this letter is due to the different quantisation axis. In the recombination hadronisation scenario of polarised

quarks, the expected value of ρ_{00} for both the magnetic field and angular momentum is also less than $1/3$ [42]. Therefore, in the presence of v_2 the spin alignment of non-prompt D^{*+} mesons due to the helicity conservation in beauty-meson decays mimics the signal of global spin alignment, expected due to the presence of large angular momentum and magnetic field in midcentral heavy-ion collisions. In the presence of additional non-flow correlations (i.e. correlations not induced by the collective expansion but rather by decays and jet contributions) [83], this effect can get further enhanced. A sizeable fraction of non-prompt D^{*+} mesons, e.g. $f_{\text{non-prompt}} = 0.2$ [72, 74] can give on the order of 5% deviation from the $\rho_{00} = 1/3$. This contribution is not negligible considering the recent J/ψ polarisation measurement in Pb–Pb collisions by the ALICE Collaboration where a deviation up to 10% from the $\rho_{00} = 1/3$ was observed [52]. Thanks to the higher luminosity and improved spatial resolution of the upgraded ITS installed in ALICE for the LHC Run 3 [84, 85], future measurements with non-prompt charm hadrons of the spin alignment in pp collisions and azimuthal anisotropy in heavy-ion collisions will provide a more accurate baseline for understanding effects induced by the initial angular momentum and magnetic field in non-central heavy-ion collisions.

5 Summary

The first measurements for prompt and non-prompt D^{*+} meson spin alignment with respect to the helicity axis at midrapidity in pp collisions at $\sqrt{s} = 13$ TeV are presented. No spin alignment is observed for the prompt D^{*+} mesons in pp collisions, with measured ρ_{00} values being consistent with $1/3$. This observation is consistent with previous measurements in e^+e^- collisions far from the Z^0 resonance and suggests that charm quarks are either produced unpolarised or their polarisation is washed out during the hadronisation process. The measured value for the non-prompt D^{*+} -meson spin density element is $\rho_{00} = 0.455 \pm 0.022(\text{stat.}) \pm 0.035(\text{syst.})$ in the $5 < p_T < 20$ GeV/ c interval. The measured value is compatible with the prediction from PYTHIA 8 + EVTGEN simulations and is interpreted as an evidence of spin alignment of non-prompt D^{*+} mesons with respect to the helicity axis due to the helicity conservation in beauty-meson decays. Based on the measurements and MC simulations, it was estimated that the spin alignment of the non-prompt D^{*+} mesons in the presence of elliptic flow can mimic the signal of global spin alignment in heavy-ion collisions. The new data presented in this letter provide an important baseline for future spin alignment measurements of D^{*+} vector mesons in heavy-ion collisions, which probe the initial angular momentum and magnetic field.

Acknowledgements

The ALICE Collaboration would like to thank all its engineers and technicians for their invaluable contributions to the construction of the experiment and the CERN accelerator teams for the outstanding performance of the LHC complex. The ALICE Collaboration gratefully acknowledges the resources and support provided by all Grid centres and the Worldwide LHC Computing Grid (WLCG) collaboration. The ALICE Collaboration acknowledges the following funding agencies for their support in building and running the ALICE detector: A. I. Alikhanyan National Science Laboratory (Yerevan Physics Institute) Foundation (ANSL), State Committee of Science and World Federation of Scientists (WFS), Armenia; Austrian Academy of Sciences, Austrian Science Fund (FWF): [M 2467-N36] and Nationalstiftung für Forschung, Technologie und Entwicklung, Austria; Ministry of Communications and High Technologies, National Nuclear Research Center, Azerbaijan; Conselho Nacional de Desenvolvimento Científico e Tecnológico (CNPq), Financiadora de Estudos e Projetos (Finep), Fundação de Amparo à Pesquisa do Estado de São Paulo (FAPESP) and Universidade Federal do Rio Grande do Sul (UFRGS), Brazil; Bulgarian Ministry of Education and Science, within the National Roadmap for Research Infrastructures 2020-2027 (object CERN), Bulgaria; Ministry of Education of China (MOEC), Ministry of Science & Technology of China (MSTC) and National Natural Science Foundation of China (NSFC), China; Ministry of Science and Education and Croatian Science

Foundation, Croatia; Centro de Aplicaciones Tecnológicas y Desarrollo Nuclear (CEADEN), Cubaenergía, Cuba; Ministry of Education, Youth and Sports of the Czech Republic, Czech Republic; The Danish Council for Independent Research | Natural Sciences, the VILLUM FONDEN and Danish National Research Foundation (DNRF), Denmark; Helsinki Institute of Physics (HIP), Finland; Commissariat à l’Energie Atomique (CEA) and Institut National de Physique Nucléaire et de Physique des Particules (IN2P3) and Centre National de la Recherche Scientifique (CNRS), France; Bundesministerium für Bildung und Forschung (BMBF) and GSI Helmholtzzentrum für Schwerionenforschung GmbH, Germany; General Secretariat for Research and Technology, Ministry of Education, Research and Religions, Greece; National Research, Development and Innovation Office, Hungary; Department of Atomic Energy Government of India (DAE), Department of Science and Technology, Government of India (DST), University Grants Commission, Government of India (UGC) and Council of Scientific and Industrial Research (CSIR), India; National Research and Innovation Agency - BRIN, Indonesia; Istituto Nazionale di Fisica Nucleare (INFN), Italy; Japanese Ministry of Education, Culture, Sports, Science and Technology (MEXT) and Japan Society for the Promotion of Science (JSPS) KAKENHI, Japan; Consejo Nacional de Ciencia (CONACYT) y Tecnología, through Fondo de Cooperación Internacional en Ciencia y Tecnología (FONCICYT) and Dirección General de Asuntos del Personal Académico (DGAPA), Mexico; Nederlandse Organisatie voor Wetenschappelijk Onderzoek (NWO), Netherlands; The Research Council of Norway, Norway; Commission on Science and Technology for Sustainable Development in the South (COMSATS), Pakistan; Pontificia Universidad Católica del Perú, Peru; Ministry of Education and Science, National Science Centre and WUT ID-UB, Poland; Korea Institute of Science and Technology Information and National Research Foundation of Korea (NRF), Republic of Korea; Ministry of Education and Scientific Research, Institute of Atomic Physics, Ministry of Research and Innovation and Institute of Atomic Physics and University Politehnica of Bucharest, Romania; Ministry of Education, Science, Research and Sport of the Slovak Republic, Slovakia; National Research Foundation of South Africa, South Africa; Swedish Research Council (VR) and Knut & Alice Wallenberg Foundation (KAW), Sweden; European Organization for Nuclear Research, Switzerland; Suranaree University of Technology (SUT), National Science and Technology Development Agency (NSTDA) and National Science, Research and Innovation Fund (NSRF via PMU-B B05F650021), Thailand; Turkish Energy, Nuclear and Mineral Research Agency (TENMAK), Turkey; National Academy of Sciences of Ukraine, Ukraine; Science and Technology Facilities Council (STFC), United Kingdom; National Science Foundation of the United States of America (NSF) and United States Department of Energy, Office of Nuclear Physics (DOE NP), United States of America. In addition, individual groups or members have received support from: European Research Council, Strong 2020 - Horizon 2020, Marie Skłodowska Curie (grant nos. 950692, 824093, 896850), European Union; Academy of Finland (Center of Excellence in Quark Matter) (grant nos. 346327, 346328), Finland; Programa de Apoyos para la Superación del Personal Académico, UNAM, Mexico.

References

- [1] L. Gladilin, “Fragmentation fractions of c and b quarks into charmed hadrons at LEP”, *Eur. Phys. J. C* **75** (2015) 19, arXiv:1404.3888 [hep-ex].
- [2] ALICE Collaboration, S. Acharya *et al.*, “Charm-quark fragmentation fractions and production cross section at midrapidity in pp collisions at the LHC”, *Phys. Rev. D* **105** (2022) L011103, arXiv:2105.06335 [nucl-ex].
- [3] LHCb Collaboration, R. Aaij *et al.*, “Measurement of B hadron fractions in 13 TeV pp collisions”, *Phys. Rev. D* **100** (2019) 031102, arXiv:1902.06794 [hep-ex].

- [4] **HFLAV** Collaboration, Y. S. Amhis *et al.*, “Averages of b-hadron, c-hadron, and τ -lepton properties as of 2018”, *Eur. Phys. J. C* **81** (2021) 226, arXiv:1909.12524 [hep-ex].
- [5] **ALICE** Collaboration, S. Acharya *et al.*, “Observation of a multiplicity dependence in the p_T -differential charm baryon-to-meson ratios in proton-proton collisions at $\sqrt{s} = 13$ TeV”, *Phys. Lett. B* **829** (2022) 137065, arXiv:2111.11948 [nucl-ex].
- [6] **ALICE** Collaboration, “First measurement of Ω_c^0 production in pp collisions at $\sqrt{s} = 13$ TeV”, *Phys. Lett. B* **846** (2023) 137625, arXiv:2205.13993 [nucl-ex].
- [7] **LHCb** Collaboration, “Evidence for modification of b quark hadronization in high-multiplicity pp collisions at $\sqrt{s} = 13$ TeV”, arXiv:2204.13042 [hep-ex].
- [8] **LHCb** Collaboration, R. Aaij *et al.*, “Precise measurement of the f_s/f_d ratio of fragmentation fractions and of B_s^0 decay branching fractions”, *Phys. Rev. D* **104** (2021) 032005, arXiv:2103.06810 [hep-ex].
- [9] A. F. Falk and M. E. Peskin, “Production, decay, and polarization of excited heavy hadrons”, *Phys. Rev. D* **49** (1994) 3320–3332, arXiv:hep-ph/9308241.
- [10] J. G. Korner, A. Pilaftsis, and M. M. Tung, “One Loop QCD Mass effects in the production of polarized bottom and top quarks”, *Z. Phys. C* **63** (1994) 575–579, arXiv:hep-ph/9311332.
- [11] T. Mannel and G. A. Schuler, “Semileptonic decays of bottom baryons at LEP”, *Phys. Lett. B* **279** (1992) 194–200.
- [12] **ALEPH** Collaboration, D. Buskulic *et al.*, “Measurement of Λ_b polarization in Z decays”, *Phys. Lett. B* **365** (1996) 437–447.
- [13] **DELPHI** Collaboration, P. Abreu *et al.*, “ Λ_b polarization in Z^0 decays at LEP”, *Phys. Lett. B* **474** (2000) 205–222.
- [14] **OPAL** Collaboration, G. Abbiendi *et al.*, “Measurement of the average polarization of b baryons in hadronic Z^0 decays”, *Phys. Lett. B* **444** (1998) 539–554, arXiv:hep-ex/9808006.
- [15] **LHCb** Collaboration, R. Aaij *et al.*, “Measurements of the $\Lambda_b^0 \rightarrow J/\psi\Lambda$ decay amplitudes and the Λ_b^0 polarisation in pp collisions at $\sqrt{s} = 7$ TeV”, *Phys. Lett. B* **724** (2013) 27–35, arXiv:1302.5578 [hep-ex].
- [16] J. F. Donoghue, “Comment on polarized fragmentation functions”, *Phys. Rev. D* **19** (1979) 2806.
- [17] I. I. Bigi, “Some quantitative estimates about final-state polarization in deep inelastic lepton-nucleon scattering”, *Nuov. Cim. A* **41** (1977) 581–591.
- [18] J. E. Augustin and F. M. Renard, “How to Measure Quark Helicities in $e + e^- \rightarrow$ Hadrons”, ECFA-LEP-49. <https://cds.cern.ch/record/867018>.
- [19] B. Andersson, G. Gustafson, G. Ingelman, and T. Sjostrand, “Parton Fragmentation and String Dynamics”, *Phys. Rept.* **97** (1983) 31–145.
- [20] T. Sjostrand, S. Mrenna, and P. Z. Skands, “PYTHIA 6.4 Physics and Manual”, *JHEP* **05** (2006) 026, arXiv:hep-ph/0603175.
- [21] T. Sjostrand *et al.*, “An introduction to PYTHIA 8.2”, *Comput. Phys. Commun.* **191** (2015) 159–177, arXiv:1410.3012 [hep-ph].

- [22] B. P. Kersevan and E. Richter-Was, “The Monte Carlo event generator AcerMC versions 2.0 to 3.8 with interfaces to PYTHIA 6.4, HERWIG 6.5 and ARIADNE 4.1”, *Comput. Phys. Commun.* **184** (2013) 919–985, arXiv:hep-ph/0405247.
- [23] J. Bellm *et al.*, “Herwig 7.0/Herwig++ 3.0 release note”, *Eur. Phys. J. C* **76** (2016) 196, arXiv:1512.01178 [hep-ph].
- [24] **DELPHI** Collaboration, P. Abreu *et al.*, “ B^* production in Z decays”, *Z. Phys. C* **68** (1995) 353–362.
- [25] **ALEPH** Collaboration, D. Buskulic *et al.*, “Production of excited beauty states in Z decays”, *Z. Phys. C* **69** (1996) 393–404.
- [26] **OPAL** Collaboration, K. Ackerstaff *et al.*, “Study of $\phi(1020)$, $D^{*\pm}$ and B^* spin alignment in hadronic Z^0 decays”, *Z. Phys. C* **74** (1997) 437–449.
- [27] **TPC/Two-Gamma** Collaboration, H. Aihara *et al.*, “Test of spin dependence in charm-quark fragmentation to D^{*} ”, *Phys. Rev. D* **43** (1991) 29–33.
- [28] **HRS** Collaboration, S. Abachi *et al.*, “Measurement of the Spin Density Matrix of D^* Mesons Produced in e^+e^- Annihilations”, *Phys. Lett. B* **199** (1987) 585–590.
- [29] **CLEO** Collaboration, Y. Kubota *et al.*, “Study of continuum D^{*+} spin alignment”, *Phys. Rev. D* **44** (1991) 593–600.
- [30] F. Becattini, F. Piccinini, and J. Rizzo, “Angular momentum conservation in heavy ion collisions at very high energy”, *Phys. Rev. C* **77** (2008) 024906, arXiv:0711.1253 [nucl-th].
- [31] D. E. Kharzeev, L. D. McLerran, and H. J. Warringa, “The Effects of topological charge change in heavy ion collisions: ‘Event by event P and CP violation’”, *Nucl. Phys.* **A803** (2008) 227–253, arXiv:0711.0950 [hep-ph].
- [32] V. Skokov, A. Y. Illarionov, and V. Toneev, “Estimate of the magnetic field strength in heavy-ion collisions”, *Int. J. Mod. Phys. A* **24** (2009) 5925–5932, arXiv:0907.1396 [nucl-th].
- [33] W.-T. Deng and X.-G. Huang, “Event-by-event generation of electromagnetic fields in heavy-ion collisions”, *Phys. Rev. C* **85** (2012) 044907, arXiv:1201.5108 [nucl-th].
- [34] P. Braun-Munzinger, V. Koch, T. Schäfer, and J. Stachel, “Properties of hot and dense matter from relativistic heavy ion collisions”, *Phys. Rept.* **621** (2016) 76–126, arXiv:1510.00442 [nucl-th].
- [35] **ALICE** Collaboration, “The ALICE experiment – A journey through QCD”, arXiv:2211.04384 [nucl-ex].
- [36] Z.-T. Liang and X.-N. Wang, “Globally polarized quark-gluon plasma in non-central A+A collisions”, *Phys. Rev. Lett.* **94** (2005) 102301, arXiv:nucl-th/0410079 [nucl-th]. [Erratum: *Phys. Rev. Lett.* **96** (2006) 039901].
- [37] P. Christakoglou, S. Qiu, and J. Staa, “Systematic study of the chiral magnetic effect with the AVFD model at LHC energies”, *Eur. Phys. J. C* **81** (2021) 717, arXiv:2106.03537 [nucl-th].
- [38] E. S. Fraga and A. J. Mizher, “Chiral transition in a strong magnetic background”, *Phys. Rev. D* **78** (2008) 025016, arXiv:0804.1452 [hep-ph].

- [39] A. Andronic *et al.*, “Heavy-flavour and quarkonium production in the LHC era: from proton–proton to heavy-ion collisions”, *Eur. Phys. J. C* **76** (2016) 107, arXiv:1506.03981 [nucl-ex].
- [40] Z.-T. Liang and X.-N. Wang, “Spin alignment of vector mesons in non-central A+A collisions”, *Phys. Lett.* **B629** (2005) 20–26, arXiv:nucl-th/0411101 [nucl-th].
- [41] Z.-T. Liang, “Global polarization of QGP in non-central heavy ion collisions at high energies”, *J. Phys.* **G34** (2007) S323–330, arXiv:0705.2852 [nucl-th].
- [42] Y.-G. Yang, R.-H. Fang, Q. Wang, and X.-N. Wang, “Quark coalescence model for polarized vector mesons and baryons”, *Phys. Rev.* **C97** (2018) 034917, arXiv:1711.06008 [nucl-th].
- [43] ALICE Collaboration, S. Acharya *et al.*, “Prompt D^0 , D^+ , and D^{*+} production in Pb–Pb collisions at $\sqrt{s_{NN}} = 5.02$ TeV”, *JHEP* **01** (2022) 174, arXiv:2110.09420 [nucl-ex].
- [44] CMS Collaboration, A. M. Sirunyan *et al.*, “Nuclear modification factor of D^0 mesons in PbPb collisions at $\sqrt{s_{NN}} = 5.02$ TeV”, *Phys. Lett. B* **782** (2018) 474–496, arXiv:1708.04962 [nucl-ex].
- [45] ALICE Collaboration, S. Acharya *et al.*, “Measurement of prompt D_s^+ -meson production and azimuthal anisotropy in Pb–Pb collisions at $\sqrt{s_{NN}}=5.02$ TeV”, *Phys. Lett. B* **827** (2022) 136986, arXiv:2110.10006 [nucl-ex].
- [46] STAR Collaboration, J. Adam *et al.*, “Observation of D_s^\pm/D^0 enhancement in Au+Au collisions at $\sqrt{s_{NN}} = 200$ GeV”, *Phys. Rev. Lett.* **127** (2021) 092301, arXiv:2101.11793 [hep-ex].
- [47] ALICE Collaboration, S. Acharya *et al.*, “Constraining hadronization mechanisms with Λ_c^+/D^0 production ratios in Pb–Pb collisions at $\sqrt{s_{NN}} = 5.02$ TeV”, *Phys. Lett. B* **839** (2023) 137796, arXiv:2112.08156 [nucl-ex].
- [48] CMS Collaboration, A. M. Sirunyan *et al.*, “Production of Λ_c^+ baryons in proton-proton and lead-lead collisions at $\sqrt{s_{NN}} = 5.02$ TeV”, *Phys. Lett. B* **803** (2020) 135328, arXiv:1906.03322 [hep-ex].
- [49] STAR Collaboration, J. Adam *et al.*, “First measurement of Λ_c baryon production in Au+Au collisions at $\sqrt{s_{NN}} = 200$ GeV”, *Phys. Rev. Lett.* **124** (2020) 172301, arXiv:1910.14628 [nucl-ex].
- [50] ALICE Collaboration, S. Acharya *et al.*, “Transverse-momentum and event-shape dependence of D-meson flow harmonics in Pb–Pb collisions at $\sqrt{s_{NN}} = 5.02$ TeV”, *Phys. Lett. B* **813** (2021) 136054, arXiv:2005.11131 [nucl-ex].
- [51] CMS Collaboration, A. M. Sirunyan *et al.*, “Measurement of prompt D^0 and \bar{D}^0 meson azimuthal anisotropy and search for strong electric fields in PbPb collisions at $\sqrt{s_{NN}} = 5.02$ TeV”, *Phys. Lett. B* **816** (2021) 136253, arXiv:2009.12628 [hep-ex].
- [52] ALICE Collaboration, “Measurement of the J/ψ polarization with respect to the event plane in Pb–Pb collisions at the LHC”, *Phys. Rev. Lett.* **131** (2023) 042303, arXiv:2204.10171 [nucl-ex].
- [53] ALICE Collaboration, S. Acharya *et al.*, “First measurement of quarkonium polarization in nuclear collisions at the LHC”, *Phys. Lett. B* **815** (2021) 136146, arXiv:2005.11128 [nucl-ex].

- [54] **Belle** Collaboration, A. Abdesselam *et al.*, “Measurement of the D^{*-} polarization in the decay $B^0 \rightarrow D^{*-} \tau^+ \nu_\tau$ ”, arXiv:1903.03102 [hep-ex].
- [55] **LHCb** Collaboration, R. Aaij *et al.*, “Angular analysis of $B^0 \rightarrow D^{*-} D_s^{*+}$ with $D_s^{*+} \rightarrow D_s^+ \gamma$ decays”, *JHEP* **06** (2021) 177, arXiv:2105.02596 [hep-ex].
- [56] M. Suzuki, “Final-state interactions and s^- quark helicity conservation in $B \rightarrow J/\psi K^*$ ”, *Phys. Rev. D* **64** (2001) 117503, arXiv:hep-ph/0106354.
- [57] **BaBar** Collaboration, B. Aubert *et al.*, “Time-Dependent and Time-Integrated Angular Analysis of $B \rightarrow \phi K_s \pi^0$ and $B \rightarrow \phi K^+ \pi^-$ ”, *Phys. Rev. D* **78** (2008) 092008, arXiv:0808.3586 [hep-ex].
- [58] U. Fano, “Description of States in Quantum Mechanics by Density Matrix and Operator Techniques”, *Rev. Mod. Phys.* **29** (1957) 74–93.
- [59] R. Snellings, “Elliptic Flow: A Brief Review”, *New J. Phys.* **13** (2011) 055008, arXiv:1102.3010 [nucl-ex].
- [60] K. Schilling, P. Seyboth, and G. E. Wolf, “On the Analysis of Vector Meson Production by Polarized Photons”, *Nucl. Phys.* **B15** (1970) 397–412. [Erratum: *Nucl. Phys. B* **18** (1970) 332].
- [61] **ALICE** Collaboration, B. B. Abelev *et al.*, “Performance of the ALICE Experiment at the CERN LHC”, *Int. J. Mod. Phys. A* **29** (2014) 1430044, arXiv:1402.4476 [nucl-ex].
- [62] **ALICE** Collaboration, K. Aamodt *et al.*, “The ALICE experiment at the CERN LHC”, *JINST* **3** (2008) S08002.
- [63] **ALICE** Collaboration, E. Abbas *et al.*, “Performance of the ALICE VZERO system”, *JINST* **8** (2013) P10016, arXiv:1306.3130 [nucl-ex].
- [64] **ALICE** Collaboration, K. Aamodt *et al.*, “Alignment of the ALICE Inner Tracking System with cosmic-ray tracks”, *JINST* **5** (2010) P03003, arXiv:1001.0502 [physics.ins-det].
- [65] **Particle Data Group** Collaboration, R. L. Workman *et al.*, “Review of Particle Physics”, *PTEP* **2022** (2022) 083C01.
- [66] J. Alme *et al.*, “The ALICE TPC, a large 3-dimensional tracking device with fast readout for ultra-high multiplicity events”, *Nucl. Instrum. Meth. A* **622** (2010) 316–367, arXiv:1001.1950 [physics.ins-det].
- [67] T. Chen and C. Guestrin, “Xgboost: A scalable tree boosting system”, *Proceedings of the 22nd ACM SIGKDD International Conference on Knowledge Discovery and Data Mining* (2016) 785–794, arXiv:1603.02754 [cs.LG].
- [68] L. Barioglio, F. Catalano, M. Concas, P. Fecchio, F. Grosa, F. Mazzaschi, and M. Puccio, “hipe4ml/hipe4ml”, July, 2021. <https://doi.org/10.5281/zenodo.5070132>.
- [69] A. Akindinov *et al.*, “Performance of the ALICE Time-Of-Flight detector at the LHC”, *Eur. Phys. J. Plus* **128** (2013) 44.
- [70] P. Skands, S. Carrazza, and J. Rojo, “Tuning PYTHIA 8.1: the Monash 2013 Tune”, *Eur. Phys. J. C* **74** (2014) 3024, arXiv:1404.5630 [hep-ph].
- [71] R. Brun, F. Bruyant, F. Carminati, S. Giani, M. Maire, A. McPherson, G. Patrick, and L. Urban, *GEANT: Detector Description and Simulation Tool; Oct 1994*. CERN Program Library. CERN, Geneva, 1993. <http://cds.cern.ch/record/1082634>. Long Writeup W5013.















- [72] **ALICE** Collaboration, S. Acharya *et al.*, “Measurement of beauty and charm production in pp collisions at $\sqrt{s} = 5.02$ TeV via non-prompt and prompt D mesons”, *JHEP* **05** (2021) 220, arXiv:2102.13601 [nucl-ex].
- [73] **ALICE** Collaboration, S. Acharya *et al.*, “First study of the two-body scattering involving charm hadrons”, *Phys. Rev. D* **106** (2022) 052010, arXiv:2201.05352 [nucl-ex].
- [74] **ALICE** Collaboration, S. Acharya *et al.*, “Measurement of beauty production via non-prompt D^0 mesons in Pb–Pb collisions at $\sqrt{s_{NN}} = 5.02$ TeV”, *JHEP* **12** (2022) 126, arXiv:2202.00815 [nucl-ex].
- [75] **CMS** Collaboration, A. M. Sirunyan *et al.*, “Studies of charm and beauty hadron long-range correlations in pp and pPb collisions at LHC energies”, *Phys. Lett. B* **813** (2021) 136036, arXiv:2009.07065 [hep-ex].
- [76] **ALICE** Collaboration, S. Acharya *et al.*, “Measurement of D-meson production at mid-rapidity in pp collisions at $\sqrt{s} = 7$ TeV”, *Eur. Phys. J. C* **77** (2017) 550, arXiv:1702.00766 [hep-ex].
- [77] D. J. Lange, “The EvtGen particle decay simulation package”, *Nucl. Instrum. Meth. A* **462** (2001) 152–155.
- [78] **ALICE** Collaboration, S. Acharya *et al.*, “D-meson azimuthal anisotropy in midcentral Pb–Pb collisions at $\sqrt{s_{NN}} = 5.02$ TeV”, *Phys. Rev. Lett.* **120** (2018) 102301, arXiv:1707.01005 [nucl-ex].
- [79] **CMS** Collaboration, A. M. Sirunyan *et al.*, “Measurement of prompt D^0 meson azimuthal anisotropy in Pb–Pb collisions at $\sqrt{s_{NN}} = 5.02$ TeV”, *Phys. Rev. Lett.* **120** (2018) 202301, arXiv:1708.03497 [nucl-ex].
- [80] **ALICE** Collaboration, S. Acharya *et al.*, “Event-shape engineering for the D-meson elliptic flow in mid-central Pb–Pb collisions at $\sqrt{s_{NN}} = 5.02$ TeV”, *JHEP* **02** (2019) 150, arXiv:1809.09371 [nucl-ex].
- [81] **ALICE** Collaboration, S. Acharya *et al.*, “Elliptic Flow of Electrons from Beauty-Hadron Decays in Pb–Pb Collisions at $\sqrt{s_{NN}} = 5.02$ TeV”, *Phys. Rev. Lett.* **126** (2021) 162001, arXiv:2005.11130 [nucl-ex].
- [82] **ATLAS** Collaboration, G. Aad *et al.*, “Measurement of azimuthal anisotropy of muons from charm and bottom hadrons in Pb–Pb collisions at $\sqrt{s_{NN}} = 5.02$ TeV with the ATLAS detector”, *Phys. Lett. B* **807** (2020) 135595, arXiv:2003.03565 [nucl-ex].
- [83] N. Borghini, P. M. Dinh, and J.-Y. Ollitrault, “Are flow measurements at SPS reliable?”, *Phys. Rev. C* **62** (2000) 034902, arXiv:nucl-th/0004026.
- [84] **ALICE** Collaboration, B. Abelev *et al.*, “Technical Design Report for the Upgrade of the ALICE Inner Tracking System”, *J. Phys. G* **41** (2014) 087002.
- [85] **ALICE** Collaboration, “ALICE upgrades during the LHC Long Shutdown 2”, arXiv:2302.01238 [physics.ins-det].

A The ALICE Collaboration

S. Acharya ¹²⁴, D. Adamová ⁸⁵, A. Adler⁶⁹, G. Aglieri Rinella ³², M. Agnello ²⁹, N. Agrawal ⁵⁰, Z. Ahammed ¹³², S. Ahmad ¹⁵, S.U. Ahn ⁷⁰, I. Ahuja ³⁷, A. Akindinov ¹⁴⁰, M. Al-Turany ⁹⁶, D. Aleksandrov ¹⁴⁰, B. Alessandro ⁵⁵, H.M. Alfanda ⁶, R. Alfaro Molina ⁶⁶, B. Ali ¹⁵, A. Alici ²⁵, N. Alizadehvandchali ¹¹³, A. Alkin ³², J. Alme ²⁰, G. Alocco ⁵¹, T. Alt ⁶³, I. Altsybeev ¹⁴⁰, M.N. Anaam ⁶, C. Andrei ⁴⁵, A. Andronic ¹³⁵, V. Anguelov ⁹³, F. Antinori ⁵³, P. Antonioli ⁵⁰, N. Apadula ⁷³, L. Aphecetche ¹⁰², H. Appelshäuser ⁶³, C. Arata ⁷², S. Arcelli ²⁵, M. Aresti ⁵¹, R. Arnaldi ⁵⁵, J.G.M.C.A. Arneiro ¹⁰⁹, I.C. Arsene ¹⁹, M. Arslanok ¹³⁷, A. Augustinus ³², R. Averbeck ⁹⁶, M.D. Azmi ¹⁵, A. Badalà ⁵², J. Bae ¹⁰³, Y.W. Baek ⁴⁰, X. Bai ¹¹⁷, R. Bailhache ⁶³, Y. Bailung ⁴⁷, A. Balbino ²⁹, A. Baldisseri ¹²⁷, B. Balis ², D. Banerjee ⁴, Z. Banoo ⁹⁰, R. Barbera ²⁶, F. Barile ³¹, L. Barioglio ⁹⁴, M. Barlou ⁷⁷, G.G. Barnaföldi ¹³⁶, L.S. Barnby ⁸⁴, V. Barret ¹²⁴, L. Barreto ¹⁰⁹, C. Bartels ¹¹⁶, K. Barth ³², E. Bartsch ⁶³, N. Bastid ¹²⁴, S. Basu ⁷⁴, G. Batigne ¹⁰², D. Battistini ⁹⁴, B. Batyunya ¹⁴¹, D. Bauri⁴⁶, J.L. Bazo Alba ¹⁰⁰, I.G. Bearden ⁸², C. Beattie ¹³⁷, P. Becht ⁹⁶, D. Behera ⁴⁷, I. Belikov ¹²⁶, A.D.C. Bell Hechavarria ¹³⁵, F. Bellini ²⁵, R. Bellwied ¹¹³, S. Belokurova ¹⁴⁰, V. Belyaev ¹⁴⁰, G. Bencedi ¹³⁶, S. Beole ²⁴, A. Bercuci ⁴⁵, Y. Berdnikov ¹⁴⁰, A. Berdnikova ⁹³, L. Bergmann ⁹³, M.G. Besoiu ⁶², L. Betev ³², P.P. Bhaduri ¹³², A. Bhasin ⁹⁰, M.A. Bhat ⁴, B. Bhattacharjee ⁴¹, L. Bianchi ²⁴, N. Bianchi ⁴⁸, J. Bielčik ³⁵, J. Bielčíková ⁸⁵, J. Biernat ¹⁰⁶, A.P. Bigot ¹²⁶, A. Bilandzic ⁹⁴, G. Biro ¹³⁶, S. Biswas ⁴, N. Bize ¹⁰², J.T. Blair ¹⁰⁷, D. Blau ¹⁴⁰, M.B. Blidaru ⁹⁶, N. Bluhme³⁸, C. Blume ⁶³, G. Boca ^{21,54}, F. Bock ⁸⁶, T. Bodova ²⁰, A. Bogdanov¹⁴⁰, S. Boi ²², J. Bok ⁵⁷, L. Boldizsár ¹³⁶, M. Bombara ³⁷, P.M. Bond ³², G. Bonomi ^{131,54}, H. Borel ¹²⁷, A. Borissov ¹⁴⁰, A.G. Borquez Carcamo ⁹³, H. Bossi ¹³⁷, E. Botta ²⁴, Y.E.M. Bouziani ⁶³, L. Bratrud ⁶³, P. Braun-Munzinger ⁹⁶, M. Bregant ¹⁰⁹, M. Broz ³⁵, G.E. Bruno ^{95,31}, M.D. Buckland ²³, D. Budnikov ¹⁴⁰, H. Buesching ⁶³, S. Bufalino ²⁹, O. Bugnon¹⁰², P. Buhler ¹⁰¹, Z. Buthelezi ^{67,120}, S.A. Bysiak¹⁰⁶, M. Cai ⁶, H. Caines ¹³⁷, A. Caliva ⁹⁶, E. Calvo Villar ¹⁰⁰, J.M.M. Camacho ¹⁰⁸, P. Camerini ²³, F.D.M. Canedo ¹⁰⁹, M. Carabas ¹²³, A.A. Carballo ³², F. Carnesecchi ³², R. Caron ¹²⁵, L.A.D. Carvalho ¹⁰⁹, J. Castillo Castellanos ¹²⁷, F. Catalano ²⁴, C. Ceballos Sanchez ¹⁴¹, I. Chakaberia ⁷³, P. Chakraborty ⁴⁶, S. Chandra ¹³², S. Chapeland ³², M. Chartier ¹¹⁶, S. Chattopadhyay ¹³², S. Chattopadhyay ⁹⁸, T.G. Chavez ⁴⁴, T. Cheng ^{96,6}, C. Cheshkov ¹²⁵, B. Cheynis ¹²⁵, V. Chibante Barroso ³², D.D. Chinellato ¹¹⁰, E.S. Chizzali ^{II,94}, J. Cho ⁵⁷, S. Cho ⁵⁷, P. Chochula ³², P. Christakoglou ⁸³, C.H. Christensen ⁸², P. Christiansen ⁷⁴, T. Chujo ¹²², M. Ciacco ²⁹, C. Cicalo ⁵¹, F. Cindolo ⁵⁰, M.R. Ciupek⁹⁶, G. Clai^{III,50}, F. Colamaria ⁴⁹, J.S. Colburn⁹⁹, D. Colella ^{95,31}, M. Colocci ³², M. Concas ^{IV,55}, G. Conesa Balbastre ⁷², Z. Conesa del Valle ¹²⁸, G. Contin ²³, J.G. Contreras ³⁵, M.L. Coquet ¹²⁷, T.M. Cormier^{I,86}, P. Cortese ^{130,55}, M.R. Cosentino ¹¹¹, F. Costa ³², S. Costanza ^{21,54}, C. Cot ¹²⁸, J. Crkovská ⁹³, P. Crochet ¹²⁴, R. Cruz-Torres ⁷³, E. Cuautle⁶⁴, P. Cui ⁶, A. Dainese ⁵³, M.C. Danisch ⁹³, A. Danu ⁶², P. Das ⁷⁹, P. Das ⁴, S. Das ⁴, A.R. Dash ¹³⁵, S. Dash ⁴⁶, R.M.H. David⁴⁴, A. De Caro ²⁸, G. de Cataldo ⁴⁹, J. de Cuveland³⁸, A. De Falco ²², D. De Gruttola ²⁸, N. De Marco ⁵⁵, C. De Martin ²³, S. De Pasquale ²⁸, S. Deb ⁴⁷, R.J. Debski ², K.R. Deja¹³³, R. Del Grande ⁹⁴, L. Dello Stritto ²⁸, W. Deng ⁶, P. Dhankher ¹⁸, D. Di Bari ³¹, A. Di Mauro ³², R.A. Diaz ^{141,7}, T. Dietel ¹¹², Y. Ding ^{125,6}, R. Divià ³², D.U. Dixit ¹⁸, Ø. Djuvsland²⁰, U. Dmitrieva ¹⁴⁰, A. Dobrin ⁶², B. Dönigus ⁶³, J.M. Dubinski ¹³³, A. Dubla ⁹⁶, S. Dudi ⁸⁹, P. Dupieux ¹²⁴, M. Durkac¹⁰⁵, N. Dzalaiova¹², T.M. Eder ¹³⁵, R.J. Ehlers ⁸⁶, V.N. Eikeland²⁰, F. Eisenhut ⁶³, D. Elia ⁴⁹, B. Erazmus ¹⁰², F. Ercolessi ²⁵, F. Erhardt ⁸⁸, M.R. Ersdal²⁰, B. Espagnon ¹²⁸, G. Eulisse ³², D. Evans ⁹⁹, S. Evdokimov ¹⁴⁰, L. Fabbietti ⁹⁴, M. Faggin ²⁷, J. Faivre ⁷², F. Fan ⁶, W. Fan ⁷³, A. Fantoni ⁴⁸, M. Fasel ⁸⁶, P. Fecchio²⁹, A. Feliciello ⁵⁵, G. Feofilov ¹⁴⁰, A. Fernández Téllez ⁴⁴, L. Ferrandi ¹⁰⁹, M.B. Ferrer ³², A. Ferrero ¹²⁷, C. Ferrero ⁵⁵, A. Ferretti ²⁴, V.J.G. Feuillard ⁹³, V. Filova ³⁵, D. Finogeev ¹⁴⁰, F.M. Fionda ⁵¹, F. Flor ¹¹³, A.N. Flores ¹⁰⁷, S. Foertsch ⁶⁷, I. Fokin ⁹³, S. Fokin ¹⁴⁰, E. Fragiaco ⁵⁶, E. Frajna ¹³⁶, U. Fuchs ³², N. Funicello ²⁸, C. Furget ⁷², A. Furs ¹⁴⁰, T. Fusayasu ⁹⁷, J.J. Gaardhøje ⁸², M. Gagliardi ²⁴, A.M. Gago ¹⁰⁰, C.D. Galvan ¹⁰⁸, D.R. Gangadharan ¹¹³, P. Ganoti ⁷⁷, C. Garabatos ⁹⁶, J.R.A. Garcia ⁴⁴, E. Garcia-Solis ⁹, K. Garg ¹⁰², C. Gargiulo ³², K. Garner¹³⁵, P. Gasik ⁹⁶, A. Gautam ¹¹⁵, M.B. Gay Ducati ⁶⁵, M. Germain ¹⁰², A. Ghimouz¹²², C. Ghosh¹³², M. Giacalone ^{50,25}, P. Giubellino ^{96,55}, P. Giubilato ²⁷, A.M.C. Glaenger ¹²⁷, P. Glässel ⁹³, E. Glimos ¹¹⁹, D.J.Q. Goh ⁷⁵, V. Gonzalez ¹³⁴, L.H. González-Trueba ⁶⁶, M. Gorgon ², S. Gotovac³³, V. Grabski ⁶⁶, L.K. Graczykowski ¹³³, E. Grecka ⁸⁵, A. Grelli ⁵⁸, C. Grigoras ³², V. Grigoriev ¹⁴⁰, S. Grigoryan ^{141,1}, F. Grosa ³², J.F. Grosse-Oetringhaus ³², R. Grosso ⁹⁶, D. Grund ³⁵, G.G. Guardiano ¹¹⁰, R. Guernane ⁷², M. Guilbaud ¹⁰², K. Gulbrandsen ⁸², T. Gündem ⁶³, T. Gunji ¹²¹, W. Guo ⁶,

A. Gupta ⁹⁰, R. Gupta ⁹⁰, S.P. Guzman ⁴⁴, L. Gyulai ¹³⁶, M.K. Habib ⁹⁶, C. Hadjidakis ¹²⁸, F.U. Haider ⁹⁰, H. Hamagaki ⁷⁵, A. Hamdi ⁷³, M. Hamid ⁶, Y. Han ¹³⁸, R. Hannigan ¹⁰⁷, M.R. Haque ¹³³, J.W. Harris ¹³⁷, A. Harton ⁹, H. Hassan ⁸⁶, D. Hatzifotiadou ⁵⁰, P. Hauer ⁴², L.B. Havener ¹³⁷, S.T. Heckel ⁹⁴, E. Hellbär ⁹⁶, H. Helstrup ³⁴, M. Hemmer ⁶³, T. Herman ³⁵, G. Herrera Corral ⁸, F. Herrmann ¹³⁵, S. Herrmann ¹²⁵, K.F. Hetland ³⁴, B. Heybeck ⁶³, H. Hillemanns ³², C. Hills ¹¹⁶, B. Hippolyte ¹²⁶, F.W. Hoffmann ⁶⁹, B. Hofman ⁵⁸, B. Hohlweger ⁸³, G.H. Hong ¹³⁸, M. Horst ⁹⁴, A. Horzyk ², Y. Hou ⁶, P. Hristov ³², C. Hughes ¹¹⁹, P. Huhn ⁶³, L.M. Huhta ¹¹⁴, C.V. Hulse ¹²⁸, T.J. Humanic ⁸⁷, A. Hutson ¹¹³, D. Hutter ³⁸, J.P. Iddon ¹¹⁶, R. Ilkaev ¹⁴⁰, H. Ilyas ¹³, M. Inaba ¹²², G.M. Innocenti ³², M. Ippolitov ¹⁴⁰, A. Isakov ⁸⁵, T. Isidori ¹¹⁵, M.S. Islam ⁹⁸, M. Ivanov ⁹⁶, M. Ivanov ¹², V. Ivanov ¹⁴⁰, M. Jablonski ², B. Jacak ⁷³, N. Jacazio ³², P.M. Jacobs ⁷³, S. Jadlovská ¹⁰⁵, J. Jadlovsky ¹⁰⁵, S. Jaelani ⁸¹, L. Jaffe ³⁸, C. Jahnke ¹¹⁰, M.J. Jakubowska ¹³³, M.A. Janik ¹³³, T. Janson ⁶⁹, M. Jercic ⁸⁸, S. Jia ¹⁰, A.A.P. Jimenez ⁶⁴, F. Jonas ⁸⁶, J.M. Jowett ^{32,96}, J. Jung ⁶³, M. Jung ⁶³, A. Junique ³², A. Jusko ⁹⁹, M.J. Kabus ^{32,133}, J. Kaewjai ¹⁰⁴, P. Kalinak ⁵⁹, A.S. Kalteyer ⁹⁶, A. Kalweit ³², V. Kaplin ¹⁴⁰, A. Karasu Uysal ⁷¹, D. Karatovic ⁸⁸, O. Karavichev ¹⁴⁰, T. Karavicheva ¹⁴⁰, P. Karczmarczyk ¹³³, E. Karpechev ¹⁴⁰, U. Keschull ⁶⁹, R. Keidel ¹³⁹, D.L.D. Keijdener ⁵⁸, M. Keil ³², B. Ketzer ⁴², A.M. Khan ⁶, S. Khan ¹⁵, A. Khanzadeev ¹⁴⁰, Y. Kharlov ¹⁴⁰, A. Khatun ^{115,15}, A. Khuntia ¹⁰⁶, M.B. Kidson ¹¹², B. Kileng ³⁴, B. Kim ¹⁶, C. Kim ¹⁶, D.J. Kim ¹¹⁴, E.J. Kim ⁶⁸, J. Kim ¹³⁸, J.S. Kim ⁴⁰, J. Kim ⁶⁸, M. Kim ^{18,93}, S. Kim ¹⁷, T. Kim ¹³⁸, K. Kimura ⁹¹, S. Kirsch ⁶³, I. Kisel ³⁸, S. Kiselev ¹⁴⁰, A. Kisiel ¹³³, J.P. Kitowski ², J.L. Klay ⁵, J. Klein ³², S. Klein ⁷³, C. Klein-Bösing ¹³⁵, M. Kleiner ⁶³, T. Klemenz ⁹⁴, A. Kluge ³², A.G. Knospe ¹¹³, C. Kobdaj ¹⁰⁴, T. Kollegger ⁹⁶, A. Kondratyev ¹⁴¹, N. Kondratyeva ¹⁴⁰, E. Kondratyuk ¹⁴⁰, J. König ⁶³, S.A. Königstorfer ⁹⁴, P.J. Konopka ³², G. Kornakov ¹³³, M. Korwieser ⁹⁴, S.D. Koryciak ², A. Kotliarov ⁸⁵, V. Kovalenko ¹⁴⁰, M. Kowalski ¹⁰⁶, V. Kozuharov ³⁶, I. Králik ⁵⁹, A. Kravčáková ³⁷, L. Kreis ⁹⁶, M. Krivda ^{99,59}, F. Krizek ⁸⁵, K. Krizkova Gajdosova ³⁵, M. Kroesen ⁹³, M. Krüger ⁶³, D.M. Krupova ³⁵, E. Kryshen ¹⁴⁰, V. Kučera ³², C. Kuhn ¹²⁶, P.G. Kuijer ⁸³, T. Kumaoka ¹²², D. Kumar ¹³², L. Kumar ⁸⁹, N. Kumar ⁸⁹, S. Kumar ³¹, S. Kundu ³², P. Kurashvili ⁷⁸, A. Kurepin ¹⁴⁰, A.B. Kurepin ¹⁴⁰, A. Kuryakin ¹⁴⁰, S. Kuschpil ⁸⁵, J. Kvapil ⁹⁹, M.J. Kweon ⁵⁷, J.Y. Kwon ⁵⁷, Y. Kwon ¹³⁸, S.L. La Pointe ³⁸, P. La Rocca ²⁶, Y.S. Lai ⁷³, A. Lakrathok ¹⁰⁴, M. Lamanna ³², R. Langoy ¹¹⁸, P. Larionov ³², E. Laudi ³², L. Lautner ^{32,94}, R. Lavicka ¹⁰¹, T. Lazareva ¹⁴⁰, R. Lea ^{131,54}, H. Lee ¹⁰³, G. Legras ¹³⁵, J. Lehrbach ³⁸, R.C. Lemmon ⁸⁴, I. León Monzón ¹⁰⁸, M.M. Lesch ⁹⁴, E.D. Lesser ¹⁸, M. Lettrich ⁹⁴, P. Lévai ¹³⁶, X. Li ¹⁰, X.L. Li ⁶, J. Lien ¹¹⁸, R. Lietava ⁹⁹, I. Likmeta ¹¹³, B. Lim ^{24,16}, S.H. Lim ¹⁶, V. Lindenstruth ³⁸, A. Lindner ⁴⁵, C. Lippmann ⁹⁶, A. Liu ¹⁸, D.H. Liu ⁶, J. Liu ¹¹⁶, I.M. Lofnes ²⁰, C. Loizides ⁸⁶, S. Lokos ¹⁰⁶, J. Lomker ⁵⁸, P. Loncar ³³, J.A. Lopez ⁹³, X. Lopez ¹²⁴, E. López Torres ⁷, P. Lu ^{96,117}, J.R. Luhder ¹³⁵, M. Lunardon ²⁷, G. Luparello ⁵⁶, Y.G. Ma ³⁹, A. Maevskaya ¹⁴⁰, M. Mager ³², T. Mahmoud ⁴², A. Maire ¹²⁶, M.V. Makariev ³⁶, M. Malaev ¹⁴⁰, G. Malfattore ²⁵, N.M. Malik ⁹⁰, Q.W. Malik ¹⁹, S.K. Malik ⁹⁰, L. Malinina ^{VII,141}, D. Mal'Kevich ¹⁴⁰, D. Mallick ⁷⁹, N. Mallick ⁴⁷, G. Mandaglio ^{30,52}, S.K. Mandal ⁷⁸, V. Manko ¹⁴⁰, F. Manso ¹²⁴, V. Manzari ⁴⁹, Y. Mao ⁶, G.V. Margagliotti ²³, A. Margotti ⁵⁰, A. Marín ⁹⁶, C. Markert ¹⁰⁷, P. Martinengo ³², J.L. Martinez ¹¹³, M.I. Martínez ⁴⁴, G. Martínez García ¹⁰², S. Masciocchi ⁹⁶, M. Masera ²⁴, A. Masoni ⁵¹, L. Massacrier ¹²⁸, A. Mastroserio ^{129,49}, O. Matonoha ⁷⁴, P.F.T. Matuoka ¹⁰⁹, A. Matyja ¹⁰⁶, C. Mayer ¹⁰⁶, A.L. Mazuecos ³², F. Mazzaschi ²⁴, M. Mazzilli ³², J.E. Mdhuli ¹²⁰, A.F. Mechler ⁶³, Y. Melikyan ^{43,140}, A. Menchaca-Rocha ⁶⁶, E. Meninno ^{101,28}, A.S. Menon ¹¹³, M. Meres ¹², S. Mhlanga ^{112,67}, Y. Miake ¹²², L. Micheletti ⁵⁵, L.C. Migliorin ¹²⁵, D.L. Mihaylov ⁹⁴, K. Mikhaylov ^{141,140}, A.N. Mishra ¹³⁶, D. Miśkowiec ⁹⁶, A. Modak ⁴, A.P. Mohanty ⁵⁸, B. Mohanty ⁷⁹, M. Mohisin Khan ^{V,15}, M.A. Molander ⁴³, Z. Moravcova ⁸², C. Mordasini ⁹⁴, D.A. Moreira De Godoy ¹³⁵, I. Morozov ¹⁴⁰, A. Morsch ³², T. Mrnjavac ³², V. Muccifora ⁴⁸, S. Muhuri ¹³², J.D. Mulligan ⁷³, A. Mulliri ²², M.G. Munhoz ¹⁰⁹, R.H. Munzer ⁶³, H. Murakami ¹²¹, S. Murray ¹¹², L. Musa ³², J. Musinsky ⁵⁹, J.W. Myrcha ¹³³, B. Naik ¹²⁰, A.I. Nambrath ¹⁸, B.K. Nandi ⁴⁶, R. Nania ⁵⁰, E. Nappi ⁴⁹, A.F. Nassirpour ⁷⁴, A. Nath ⁹³, C. Nattrass ¹¹⁹, M.N. Naydenov ³⁶, A. Neagu ¹⁹, A. Negru ¹²³, L. Nellen ⁶⁴, S.V. Nesbo ³⁴, G. Neskovic ³⁸, D. Nesterov ¹⁴⁰, B.S. Nielsen ⁸², E.G. Nielsen ⁸², S. Nikolaev ¹⁴⁰, S. Nikulin ¹⁴⁰, V. Nikulin ¹⁴⁰, F. Noferini ⁵⁰, S. Noh ¹¹, P. Nomokonov ¹⁴¹, J. Norman ¹¹⁶, N. Novitzky ¹²², P. Nowakowski ¹³³, A. Nyanin ¹⁴⁰, J. Nystrand ²⁰, M. Ogino ⁷⁵, A. Ohlson ⁷⁴, V.A. Okorokov ¹⁴⁰, J. Oliński ¹³³, A.C. Oliveira Da Silva ¹¹⁹, M.H. Oliver ¹³⁷, A. Onnerstad ¹¹⁴, C. Oppedisano ⁵⁵, A. Ortiz Velasquez ⁶⁴, J. Otwinowski ¹⁰⁶, M. Oya ⁹¹, K. Oyama ⁷⁵, Y. Pachmayer ⁹³, S. Padhan ⁴⁶, D. Pagano ^{131,54}, G. Pačić ⁶⁴, A. Palasciano ⁴⁹,

S. Panebianco ¹²⁷, H. Park ¹²², H. Park ¹⁰³, J. Park ⁵⁷, J.E. Parkkila ³², R.N. Patra⁹⁰, B. Paul ²², H. Pei ⁶, T. Peitzmann ⁵⁸, X. Peng ⁶, M. Pennisi ²⁴, L.G. Pereira ⁶⁵, D. Peresunko ¹⁴⁰, G.M. Perez ⁷, S. Perrin ¹²⁷, Y. Pestov¹⁴⁰, V. Petráček ³⁵, V. Petrov ¹⁴⁰, M. Petrovici ⁴⁵, R.P. Pezzi ^{102,65}, S. Piano ⁵⁶, M. Pikna ¹², P. Pillot ¹⁰², O. Pinazza ^{50,32}, L. Pinsky¹¹³, C. Pinto ⁹⁴, S. Pisano ⁴⁸, M. Płoskoń ⁷³, M. Planinic⁸⁸, F. Pliquett⁶³, M.G. Poghosyan ⁸⁶, B. Polichtchouk ¹⁴⁰, S. Politano ²⁹, N. Poljak ⁸⁸, A. Pop ⁴⁵, S. Porteboeuf-Houssais ¹²⁴, V. Pozdniakov ¹⁴¹, K.K. Pradhan ⁴⁷, S.K. Prasad ⁴, S. Prasad ⁴⁷, R. Preghenella ⁵⁰, F. Prino ⁵⁵, C.A. Pruneau ¹³⁴, I. Pshenichnov ¹⁴⁰, M. Puccio ³², S. Pucillo ²⁴, Z. Pugelova¹⁰⁵, S. Qiu ⁸³, L. Quaglia ²⁴, R.E. Quishpe¹¹³, S. Ragoni ^{14,99}, A. Rakotozafindrabe ¹²⁷, L. Ramello ^{130,55}, F. Rami ¹²⁶, S.A.R. Ramirez ⁴⁴, T.A. Rancien⁷², M. Rasa ²⁶, S.S. Räsänen ⁴³, R. Rath ⁵⁰, M.P. Rauch ²⁰, I. Ravasenga ⁸³, K.F. Read ^{86,119}, C. Reckziegel ¹¹¹, A.R. Redelbach ³⁸, K. Redlich ^{VI,78}, C.A. Reetz ⁹⁶, A. Rehman²⁰, F. Reidt ³², H.A. Reme-Ness ³⁴, Z. Rescakova³⁷, K. Reygers ⁹³, A. Riabov ¹⁴⁰, V. Riabov ¹⁴⁰, R. Ricci ²⁸, M. Richter ¹⁹, A.A. Riedel ⁹⁴, W. Riegler ³², C. Ristea ⁶², M. Rodríguez Cahuantzi ⁴⁴, K. Røed ¹⁹, R. Rogalev ¹⁴⁰, E. Rogochaya ¹⁴¹, T.S. Rogoschinski ⁶³, D. Rohr ³², D. Röhrich ²⁰, P.F. Rojas⁴⁴, S. Rojas Torres ³⁵, P.S. Rokita ¹³³, G. Romanenko ¹⁴¹, F. Ronchetti ⁴⁸, A. Rosano ^{30,52}, E.D. Rosas⁶⁴, K. Roslon ¹³³, A. Rossi ⁵³, A. Roy ⁴⁷, S. Roy ⁴⁶, N. Rubini ²⁵, D. Ruggiano ¹³³, R. Rui ²³, B. Rumyantsev¹⁴¹, P.G. Russek ², R. Russo ⁸³, A. Rustamov ⁸⁰, E. Ryabinkin ¹⁴⁰, Y. Ryabov ¹⁴⁰, A. Rybicki ¹⁰⁶, H. Rytkonen ¹¹⁴, W. Rzesza ¹³³, O.A.M. Saarimaki ⁴³, R. Sadek ¹⁰², S. Sadhu ³¹, S. Sadovsky ¹⁴⁰, J. Saetre ²⁰, K. Šafařík ³⁵, S.K. Saha ⁴, S. Saha ⁷⁹, B. Sahoo ⁴⁶, R. Sahoo ⁴⁷, S. Sahoo⁶⁰, D. Sahu ⁴⁷, P.K. Sahu ⁶⁰, J. Saini ¹³², K. Sajdakova³⁷, S. Sakai ¹²², M.P. Salvan ⁹⁶, S. Sambyal ⁹⁰, I. Sanna ^{32,94}, T.B. Saramela¹⁰⁹, D. Sarkar ¹³⁴, N. Sarkar¹³², P. Sarma ⁴¹, V. Sarritzu ²², V.M. Sarti ⁹⁴, M.H.P. Sas ¹³⁷, J. Schambach ⁸⁶, H.S. Scheid ⁶³, C. Schiaua ⁴⁵, R. Schicker ⁹³, A. Schmah⁹³, C. Schmidt ⁹⁶, H.R. Schmidt⁹², M.O. Schmidt ³², M. Schmidt⁹², N.V. Schmidt ⁸⁶, A.R. Schmier ¹¹⁹, R. Schotter ¹²⁶, A. Schröter ³⁸, J. Schukraft ³², K. Schwarz⁹⁶, K. Schweda ⁹⁶, G. Scioli ²⁵, E. Scomparin ⁵⁵, J.E. Seger ¹⁴, Y. Sekiguchi¹²¹, D. Sekihata ¹²¹, I. Selyuzhenkov ^{96,140}, S. Senyukov ¹²⁶, J.J. Seo ⁵⁷, D. Serebryakov ¹⁴⁰, L. Šerkšnytė ⁹⁴, A. Sevcenco ⁶², T.J. Shaba ⁶⁷, A. Shabetai ¹⁰², R. Shahoyan³², A. Shangaraev ¹⁴⁰, A. Sharma⁸⁹, B. Sharma ⁹⁰, D. Sharma ⁴⁶, H. Sharma ¹⁰⁶, M. Sharma ⁹⁰, S. Sharma ⁷⁵, S. Sharma ⁹⁰, U. Sharma ⁹⁰, A. Shatat ¹²⁸, O. Sheibani¹¹³, K. Shigaki ⁹¹, M. Shimomura⁷⁶, J. Shin¹¹, S. Shirinkin ¹⁴⁰, Q. Shou ³⁹, Y. Sibirjak ¹⁴⁰, S. Siddhanta ⁵¹, T. Siemiarczuk ⁷⁸, T.F. Silva ¹⁰⁹, D. Silvermyr ⁷⁴, T. Simantathammakul¹⁰⁴, R. Simeonov ³⁶, B. Singh⁹⁰, B. Singh ⁹⁴, R. Singh ⁷⁹, R. Singh ⁹⁰, R. Singh ⁴⁷, S. Singh ¹⁵, V.K. Singh ¹³², V. Singhal ¹³², T. Sinha ⁹⁸, B. Sitar ¹², M. Sitta ^{130,55}, T.B. Skaali¹⁹, G. Skorodumovs ⁹³, M. Slupecki ⁴³, N. Smirnov ¹³⁷, R.J.M. Snellings ⁵⁸, E.H. Solheim ¹⁹, J. Song ¹¹³, A. Songmoolnak¹⁰⁴, F. Soramel ²⁷, R. Spijkers ⁸³, I. Sputowska ¹⁰⁶, J. Staa ⁷⁴, J. Stachel ⁹³, I. Stan ⁶², P.J. Steffanic ¹¹⁹, S.F. Stiefelmaier ⁹³, D. Stocco ¹⁰², I. Storehaug ¹⁹, P. Stratmann ¹³⁵, S. Strazzi ²⁵, C.P. Stylianidis⁸³, A.A.P. Suaide ¹⁰⁹, C. Suire ¹²⁸, M. Sukhanov ¹⁴⁰, M. Suljic ³², R. Sultanov ¹⁴⁰, V. Sumberia ⁹⁰, S. Sumowidagdo ⁸¹, S. Swain⁶⁰, I. Szarka ¹², M. Szymkowski ¹³³, S.F. Taghavi ⁹⁴, G. TAILLEPIED ⁹⁶, J. Takahashi ¹¹⁰, G.J. Tambave ²⁰, S. Tang ^{124,6}, Z. Tang ¹¹⁷, J.D. Tapia Takaki ¹¹⁵, N. Tapus¹²³, L.A. Tarasovicova ¹³⁵, M.G. Tarzila ⁴⁵, G.F. Tassielli ³¹, A. Tauro ³², G. Tejada Muñoz ⁴⁴, A. Telesca ³², L. Terlizzi ²⁴, C. Terrevoli ¹¹³, G. Tersimonov³, S. Thakur ⁴, D. Thomas ¹⁰⁷, A. Tikhonov ¹⁴⁰, A.R. Timmins ¹¹³, M. Tkacik¹⁰⁵, T. Tkacik ¹⁰⁵, A. Toia ⁶³, R. Tokumoto⁹¹, N. Topilskaya ¹⁴⁰, M. Toppi ⁴⁸, F. Torales-Acosta¹⁸, T. Tork ¹²⁸, A.G. Torres Ramos ³¹, A. Trifiró ^{30,52}, A.S. Triolo ^{30,52}, S. Tripathy ⁵⁰, T. Tripathy ⁴⁶, S. Trogolo ³², V. Trubnikov ³, W.H. Trzaska ¹¹⁴, T.P. Trzcinski ¹³³, A. Tumkin ¹⁴⁰, R. Turrisi ⁵³, T.S. Tveter ¹⁹, K. Ullaland ²⁰, B. Ulukutlu ⁹⁴, A. Uras ¹²⁵, M. Urioni ^{54,131}, G.L. Usai ²², M. Vala³⁷, N. Valle ²¹, L.V.R. van Doremalen⁵⁸, M. van Leeuwen ⁸³, C.A. van Veen ⁹³, R.J.G. van Weelden ⁸³, P. Vande Vyvre ³², D. Varga ¹³⁶, Z. Varga ¹³⁶, M. Vasileiou ⁷⁷, A. Vasiliev ¹⁴⁰, O. Vázquez Doce ⁴⁸, O. Vazquez Rueda ^{113,74}, V. Vechernin ¹⁴⁰, E. Vercellin ²⁴, S. Vergara Limón⁴⁴, L. Vermunt ⁹⁶, R. Vértesi ¹³⁶, M. Verweij ⁵⁸, L. Vickovic³³, Z. Vilakazi¹²⁰, O. Villalobos Baillie ⁹⁹, A. Villani ²³, G. VINO ⁴⁹, A. Vinogradov ¹⁴⁰, T. Virgili ²⁸, V. Vislavicius⁷⁴, A. Vodopyanov ¹⁴¹, B. Volkel ³², M.A. Völkl ⁹³, K. Voloshin¹⁴⁰, S.A. Voloshin ¹³⁴, G. Volpe ³¹, B. von Haller ³², I. Vorobyev ⁹⁴, N. Vozniuk ¹⁴⁰, J. Vrláková³⁷, C. Wang ³⁹, D. Wang³⁹, Y. Wang ³⁹, A. Wegrzynek ³², F.T. Weiglhofer³⁸, S.C. Wenzel ³², J.P. Wessels ¹³⁵, S.L. Weyhmilller ¹³⁷, J. Wiechula ⁶³, J. Wikne ¹⁹, G. Wilk ⁷⁸, J. Wilkinson ⁹⁶, G.A. Willems ¹³⁵, B. Windelband ⁹³, M. Winn ¹²⁷, J.R. Wright ¹⁰⁷, W. Wu³⁹, Y. Wu ¹¹⁷, R. Xu ⁶, A. Yadav ⁴², A.K. Yadav ¹³², S. Yalcin ⁷¹, Y. Yamaguchi ⁹¹, S. Yang²⁰, S. Yano ⁹¹, Z. Yin ⁶, I.-K. Yoo ¹⁶, J.H. Yoon ⁵⁷, S. Yuan²⁰, A. Yuncu ⁹³, V. Zaccolo ²³, C. Zampolli ³², F. Zanone ⁹³, N. Zardoshti ^{32,99}, A. Zarochentsev ¹⁴⁰,

P. Závada ⁶¹, N. Zaviyalov¹⁴⁰, M. Zhalov ¹⁴⁰, B. Zhang ⁶, L. Zhang ³⁹, S. Zhang ³⁹, X. Zhang ⁶,
 Y. Zhang¹¹⁷, Z. Zhang ⁶, M. Zhao ¹⁰, V. Zherebchevskii ¹⁴⁰, Y. Zhi¹⁰, D. Zhou ⁶, Y. Zhou ⁸²,
 J. Zhu ^{96,6}, Y. Zhu⁶, S.C. Zugravel ⁵⁵, N. Zurlo ^{131,54}

Affiliation Notes

^I Deceased

^{II} Also at: Max-Planck-Institut für Physik, Munich, Germany

^{III} Also at: Italian National Agency for New Technologies, Energy and Sustainable Economic Development (ENEA), Bologna, Italy

^{IV} Also at: Dipartimento DET del Politecnico di Torino, Turin, Italy

^V Also at: Department of Applied Physics, Aligarh Muslim University, Aligarh, India

^{VI} Also at: Institute of Theoretical Physics, University of Wrocław, Poland

^{VII} Also at: An institution covered by a cooperation agreement with CERN

Collaboration Institutes

¹ A.I. Alikhanyan National Science Laboratory (Yerevan Physics Institute) Foundation, Yerevan, Armenia

² AGH University of Krakow, Cracow, Poland

³ Bogolyubov Institute for Theoretical Physics, National Academy of Sciences of Ukraine, Kiev, Ukraine

⁴ Bose Institute, Department of Physics and Centre for Astroparticle Physics and Space Science (CAPSS), Kolkata, India

⁵ California Polytechnic State University, San Luis Obispo, California, United States

⁶ Central China Normal University, Wuhan, China

⁷ Centro de Aplicaciones Tecnológicas y Desarrollo Nuclear (CEADEN), Havana, Cuba

⁸ Centro de Investigación y de Estudios Avanzados (CINVESTAV), Mexico City and Mérida, Mexico

⁹ Chicago State University, Chicago, Illinois, United States

¹⁰ China Institute of Atomic Energy, Beijing, China

¹¹ Chungbuk National University, Cheongju, Republic of Korea

¹² Comenius University Bratislava, Faculty of Mathematics, Physics and Informatics, Bratislava, Slovak Republic

¹³ COMSATS University Islamabad, Islamabad, Pakistan

¹⁴ Creighton University, Omaha, Nebraska, United States

¹⁵ Department of Physics, Aligarh Muslim University, Aligarh, India

¹⁶ Department of Physics, Pusan National University, Pusan, Republic of Korea

¹⁷ Department of Physics, Sejong University, Seoul, Republic of Korea

¹⁸ Department of Physics, University of California, Berkeley, California, United States

¹⁹ Department of Physics, University of Oslo, Oslo, Norway

²⁰ Department of Physics and Technology, University of Bergen, Bergen, Norway

²¹ Dipartimento di Fisica, Università di Pavia, Pavia, Italy

²² Dipartimento di Fisica dell'Università and Sezione INFN, Cagliari, Italy

²³ Dipartimento di Fisica dell'Università and Sezione INFN, Trieste, Italy

²⁴ Dipartimento di Fisica dell'Università and Sezione INFN, Turin, Italy

²⁵ Dipartimento di Fisica e Astronomia dell'Università and Sezione INFN, Bologna, Italy

²⁶ Dipartimento di Fisica e Astronomia dell'Università and Sezione INFN, Catania, Italy

²⁷ Dipartimento di Fisica e Astronomia dell'Università and Sezione INFN, Padova, Italy

²⁸ Dipartimento di Fisica 'E.R. Caianiello' dell'Università and Gruppo Collegato INFN, Salerno, Italy

²⁹ Dipartimento DISAT del Politecnico and Sezione INFN, Turin, Italy

³⁰ Dipartimento di Scienze MIFT, Università di Messina, Messina, Italy

³¹ Dipartimento Interateneo di Fisica 'M. Merlin' and Sezione INFN, Bari, Italy

³² European Organization for Nuclear Research (CERN), Geneva, Switzerland

³³ Faculty of Electrical Engineering, Mechanical Engineering and Naval Architecture, University of Split, Split, Croatia

³⁴ Faculty of Engineering and Science, Western Norway University of Applied Sciences, Bergen, Norway

³⁵ Faculty of Nuclear Sciences and Physical Engineering, Czech Technical University in Prague, Prague, Czech Republic

³⁶ Faculty of Physics, Sofia University, Sofia, Bulgaria

- ³⁷ Faculty of Science, P.J. Šafárik University, Košice, Slovak Republic
³⁸ Frankfurt Institute for Advanced Studies, Johann Wolfgang Goethe-Universität Frankfurt, Frankfurt, Germany
³⁹ Fudan University, Shanghai, China
⁴⁰ Gangneung-Wonju National University, Gangneung, Republic of Korea
⁴¹ Gauhati University, Department of Physics, Guwahati, India
⁴² Helmholtz-Institut für Strahlen- und Kernphysik, Rheinische Friedrich-Wilhelms-Universität Bonn, Bonn, Germany
⁴³ Helsinki Institute of Physics (HIP), Helsinki, Finland
⁴⁴ High Energy Physics Group, Universidad Autónoma de Puebla, Puebla, Mexico
⁴⁵ Horia Hulubei National Institute of Physics and Nuclear Engineering, Bucharest, Romania
⁴⁶ Indian Institute of Technology Bombay (IIT), Mumbai, India
⁴⁷ Indian Institute of Technology Indore, Indore, India
⁴⁸ INFN, Laboratori Nazionali di Frascati, Frascati, Italy
⁴⁹ INFN, Sezione di Bari, Bari, Italy
⁵⁰ INFN, Sezione di Bologna, Bologna, Italy
⁵¹ INFN, Sezione di Cagliari, Cagliari, Italy
⁵² INFN, Sezione di Catania, Catania, Italy
⁵³ INFN, Sezione di Padova, Padova, Italy
⁵⁴ INFN, Sezione di Pavia, Pavia, Italy
⁵⁵ INFN, Sezione di Torino, Turin, Italy
⁵⁶ INFN, Sezione di Trieste, Trieste, Italy
⁵⁷ Inha University, Incheon, Republic of Korea
⁵⁸ Institute for Gravitational and Subatomic Physics (GRASP), Utrecht University/Nikhef, Utrecht, Netherlands
⁵⁹ Institute of Experimental Physics, Slovak Academy of Sciences, Košice, Slovak Republic
⁶⁰ Institute of Physics, Homi Bhabha National Institute, Bhubaneswar, India
⁶¹ Institute of Physics of the Czech Academy of Sciences, Prague, Czech Republic
⁶² Institute of Space Science (ISS), Bucharest, Romania
⁶³ Institut für Kernphysik, Johann Wolfgang Goethe-Universität Frankfurt, Frankfurt, Germany
⁶⁴ Instituto de Ciencias Nucleares, Universidad Nacional Autónoma de México, Mexico City, Mexico
⁶⁵ Instituto de Física, Universidade Federal do Rio Grande do Sul (UFRGS), Porto Alegre, Brazil
⁶⁶ Instituto de Física, Universidad Nacional Autónoma de México, Mexico City, Mexico
⁶⁷ iThemba LABS, National Research Foundation, Somerset West, South Africa
⁶⁸ Jeonbuk National University, Jeonju, Republic of Korea
⁶⁹ Johann-Wolfgang-Goethe Universität Frankfurt Institut für Informatik, Fachbereich Informatik und Mathematik, Frankfurt, Germany
⁷⁰ Korea Institute of Science and Technology Information, Daejeon, Republic of Korea
⁷¹ KTO Karatay University, Konya, Turkey
⁷² Laboratoire de Physique Subatomique et de Cosmologie, Université Grenoble-Alpes, CNRS-IN2P3, Grenoble, France
⁷³ Lawrence Berkeley National Laboratory, Berkeley, California, United States
⁷⁴ Lund University Department of Physics, Division of Particle Physics, Lund, Sweden
⁷⁵ Nagasaki Institute of Applied Science, Nagasaki, Japan
⁷⁶ Nara Women's University (NWU), Nara, Japan
⁷⁷ National and Kapodistrian University of Athens, School of Science, Department of Physics, Athens, Greece
⁷⁸ National Centre for Nuclear Research, Warsaw, Poland
⁷⁹ National Institute of Science Education and Research, Homi Bhabha National Institute, Jatni, India
⁸⁰ National Nuclear Research Center, Baku, Azerbaijan
⁸¹ National Research and Innovation Agency - BRIN, Jakarta, Indonesia
⁸² Niels Bohr Institute, University of Copenhagen, Copenhagen, Denmark
⁸³ Nikhef, National institute for subatomic physics, Amsterdam, Netherlands
⁸⁴ Nuclear Physics Group, STFC Daresbury Laboratory, Daresbury, United Kingdom
⁸⁵ Nuclear Physics Institute of the Czech Academy of Sciences, Husinec-Řež, Czech Republic
⁸⁶ Oak Ridge National Laboratory, Oak Ridge, Tennessee, United States
⁸⁷ Ohio State University, Columbus, Ohio, United States
⁸⁸ Physics department, Faculty of science, University of Zagreb, Zagreb, Croatia
⁸⁹ Physics Department, Panjab University, Chandigarh, India

- ⁹⁰ Physics Department, University of Jammu, Jammu, India
⁹¹ Physics Program and International Institute for Sustainability with Knotted Chiral Meta Matter (SKCM2), Hiroshima University, Hiroshima, Japan
⁹² Physikalisches Institut, Eberhard-Karls-Universität Tübingen, Tübingen, Germany
⁹³ Physikalisches Institut, Ruprecht-Karls-Universität Heidelberg, Heidelberg, Germany
⁹⁴ Physik Department, Technische Universität München, Munich, Germany
⁹⁵ Politecnico di Bari and Sezione INFN, Bari, Italy
⁹⁶ Research Division and ExtreMe Matter Institute EMMI, GSI Helmholtzzentrum für Schwerionenforschung GmbH, Darmstadt, Germany
⁹⁷ Saga University, Saga, Japan
⁹⁸ Saha Institute of Nuclear Physics, Homi Bhabha National Institute, Kolkata, India
⁹⁹ School of Physics and Astronomy, University of Birmingham, Birmingham, United Kingdom
¹⁰⁰ Sección Física, Departamento de Ciencias, Pontificia Universidad Católica del Perú, Lima, Peru
¹⁰¹ Stefan Meyer Institut für Subatomare Physik (SMI), Vienna, Austria
¹⁰² SUBATECH, IMT Atlantique, Nantes Université, CNRS-IN2P3, Nantes, France
¹⁰³ Sungkyunkwan University, Suwon City, Republic of Korea
¹⁰⁴ Suranaree University of Technology, Nakhon Ratchasima, Thailand
¹⁰⁵ Technical University of Košice, Košice, Slovak Republic
¹⁰⁶ The Henryk Niewodniczanski Institute of Nuclear Physics, Polish Academy of Sciences, Cracow, Poland
¹⁰⁷ The University of Texas at Austin, Austin, Texas, United States
¹⁰⁸ Universidad Autónoma de Sinaloa, Culiacán, Mexico
¹⁰⁹ Universidade de São Paulo (USP), São Paulo, Brazil
¹¹⁰ Universidade Estadual de Campinas (UNICAMP), Campinas, Brazil
¹¹¹ Universidade Federal do ABC, Santo Andre, Brazil
¹¹² University of Cape Town, Cape Town, South Africa
¹¹³ University of Houston, Houston, Texas, United States
¹¹⁴ University of Jyväskylä, Jyväskylä, Finland
¹¹⁵ University of Kansas, Lawrence, Kansas, United States
¹¹⁶ University of Liverpool, Liverpool, United Kingdom
¹¹⁷ University of Science and Technology of China, Hefei, China
¹¹⁸ University of South-Eastern Norway, Kongsberg, Norway
¹¹⁹ University of Tennessee, Knoxville, Tennessee, United States
¹²⁰ University of the Witwatersrand, Johannesburg, South Africa
¹²¹ University of Tokyo, Tokyo, Japan
¹²² University of Tsukuba, Tsukuba, Japan
¹²³ University Politehnica of Bucharest, Bucharest, Romania
¹²⁴ Université Clermont Auvergne, CNRS/IN2P3, LPC, Clermont-Ferrand, France
¹²⁵ Université de Lyon, CNRS/IN2P3, Institut de Physique des 2 Infinis de Lyon, Lyon, France
¹²⁶ Université de Strasbourg, CNRS, IPHC UMR 7178, F-67000 Strasbourg, France, Strasbourg, France
¹²⁷ Université Paris-Saclay, Centre d'Etudes de Saclay (CEA), IRFU, Département de Physique Nucléaire (DPhN), Saclay, France
¹²⁸ Université Paris-Saclay, CNRS/IN2P3, IJCLab, Orsay, France
¹²⁹ Università degli Studi di Foggia, Foggia, Italy
¹³⁰ Università del Piemonte Orientale, Vercelli, Italy
¹³¹ Università di Brescia, Brescia, Italy
¹³² Variable Energy Cyclotron Centre, Homi Bhabha National Institute, Kolkata, India
¹³³ Warsaw University of Technology, Warsaw, Poland
¹³⁴ Wayne State University, Detroit, Michigan, United States
¹³⁵ Westfälische Wilhelms-Universität Münster, Institut für Kernphysik, Münster, Germany
¹³⁶ Wigner Research Centre for Physics, Budapest, Hungary
¹³⁷ Yale University, New Haven, Connecticut, United States
¹³⁸ Yonsei University, Seoul, Republic of Korea
¹³⁹ Zentrum für Technologie und Transfer (ZTT), Worms, Germany
¹⁴⁰ Affiliated with an institute covered by a cooperation agreement with CERN
¹⁴¹ Affiliated with an international laboratory covered by a cooperation agreement with CERN.